NASA TR R-55

NATIONAL AERONAUTICS AND SPACE ADMINISTRATION

TECHNICAL REPORT
R-55

AN ANALYSIS OF THE CORRIDOR AND GUIDANCE REQUIREMENTS FOR SUPERCIRCULAR ENTRY INTO PLANETARY ATMOSPHERES

By DEAN R. CHAPMAN

1960

For sale by the Superintendent of Documents, U.S. Government Printing Office, Washington 25, D.C. Yearly subscription, $15; foreign, $19; single copy price varies according to size ---------- Price 50 cents

TECHNICAL REPORT R-55

AN ANALYSIS OF THE CORRIDOR AND GUIDANCE REQUIREMENTS FOR SUPERCIRCULAR ENTRY INTO PLANETARY ATMOSPHERES

By DEAN R. CHAPMAN

Ames Research Center
Moffett Field, Calif.

TECHNICAL REPORT R-55

AN ANALYSIS OF THE CORRIDOR AND GUIDANCE REQUIREMENTS FOR SUPERCIRCULAR ENTRY INTO PLANETARY ATMOSPHERES

By Dean R. Chapman

SUMMARY

An analysis is presented of supercircular entry into a planet's atmosphere giving particular attention to the corridor through which spacecraft must be guided in order to accomplish various maneuvers. A dimensionless parameter based on conditions at the conic perigee altitude is introduced for characterizing supercircular entries and conveniently prescribing corridor widths associated with elliptic, parabolic, or hyperbolic approach trajectories. The analysis applies to vehicles of arbitrary weight, shape, and size. Illustrative calculations are made for Venus, Earth, Mars, Jupiter, and Titan.

For nonlifting vehicles having fixed aerodynamic coefficients, curves are presented of dimensionless parameters from which can be calculated the maximum deceleration, maximum rate of laminar convective heating, and total laminar heat absorbed during single-pass entry at velocities up to twice circular velocity. For lifting vehicles, curves are presented of the maximum deceleration and overshoot boundary of an entry corridor; equations are presented for estimating laminar aerodynamic heating from the maximum deceleration. It is shown that the corridor width is independent of vehicle weight, dimensions, and drag coefficient, provided these are the same at the overshoot boundary as at undershoot. The corridors of certain planets can be broadened markedly by the application of aerodynamic lift; for example, the 10-earth-g corridor width for single-pass, nonlifting, parabolic entry is increased from 0 miles for Jupiter, 7 for Earth, and 8 for Venus, to 52, 51, and 52 miles, respectively, by employing a lift-drag ratio of 1. The use of aerodynamic lift does not increase appreciably the corridors of Mars and Titan. All corridor widths decrease rapidly as the entry velocity is increased.

Terminal guidance requirements on accuracy of velocity and flight path angle for successfully entering various corridors are compared with analogous requirements for putting a satellite into orbit, for hitting the moon from the earth, and for achieving ICBM accuracy. Consideration is given to the terminal guidance problem involved in using a planet's atmosphere—rather than rocket fuel—to effect orbital transfers from heliocentric to planetocentric motion, thereby converting a hyperbolic approach trajectory to an elliptic orbit about the target planet. This fuel saving maneuver appears technologically feasible for certain planetary voyages, and implies the possibility of achieving a large reduction in required Earth lift-off weight of chemical propulsion systems.

INTRODUCTION

The motion and heating during entry into an atmosphere at supercircular velocity has been studied less extensively than that at circular velocity. At present, entry at circular velocity is of more immediate practical concern, since the first manned space capsules are to be launched in near-circular orbits. In the hopefully near future, though, supercircular entry at essentially parabolic velocity ($\sqrt{2}$ times circular velocity) will be of practical concern upon return from the Moon. In the more distant future, entry at hyperbolic velocity (greater than $\sqrt{2}$ times circular velocity) will undoubtedly also be of practical interest, especially in connection with interplanetary flight. Hyperbolic entry with atmosphere braking can effect an orbital transfer from heliocentric to planetocentric motion without the expenditure of fuel, thereby making possible large reductions in Earth lift-off weight for many interplanetary missions.

An important problem for supercircular entries, which is relatively unimportant for near-circular entries, is that of the guidance accuracy required in order to accomplish a desired entry maneuver, such as completing entry on a single pass without

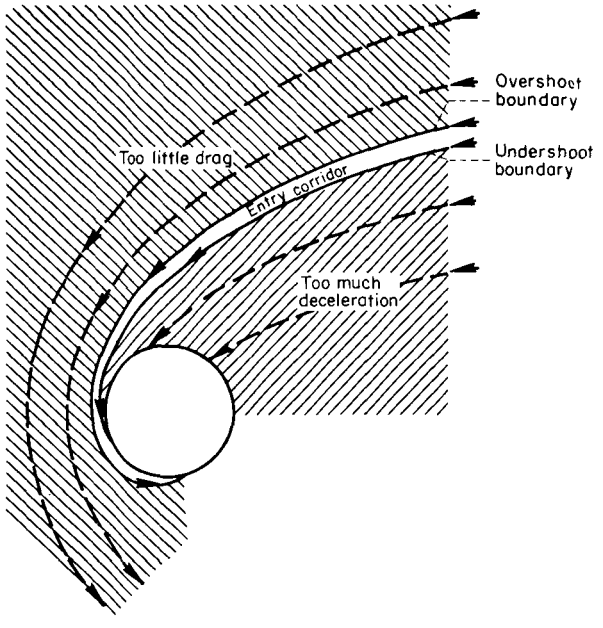

encountering excessive deceleration or heating conditions during entry. Terrestrial flight is tolerant of guidance errors accompanying a landing approach, since an undershoot is readily corrected by a brief application of power, and an overshoot by a return approach. Space flight, in contradistinction, is unforgiving of guidance errors, since undershoot may cause destruction of the vehicle during entry, and, in a hyperbolic approach, overshoot may result in a homeless exit into space. If the guidance error results in undershooting an intended trajectory too much, as illustrated by the inner two dashed trajectories in the adjacent sketch, the vehicle will enter the atmosphere at an excessively steep angle, thereby experiencing either too much deceleration for the occupants and/or spacecraft, or perhaps too much deceleration for the desired maneuver. If the guidance error results in overshooting the intended trajectory too much, as illustrated by the outer two dashed trajectories, the vehicle will not encounter enough atmosphere for slowing sufficiently either to complete entry in a single pass, or to effect a particular orbital transfer. Hence the shaded portions representing excessive overshoot and undershoot in the sketch are excluded as not representing the intended entry maneuver. For some planets, all that is left is a meagerly narrow corridor through which the vehicle must be guided. The outer and inner boundaries of this entry corridor are referred to herein as the overshoot and undershoot boundaries, respectively.

The object of the present report is to make a general study of the entry corridor and its boundaries, giving consideration to aerodynamic heating problems for various lift-drag ratios, entry velocities, and planets, and to the guidance problem which the corridor imposes. A novel feature of the present analysis is the introduction of a dimensionless perigee parameter combining certain characteristics of the vehicle with certain quantities associated with the conic perigee altitude. By conic perigee is meant that fictitious perigee point through which a drag-free entry trajectory would pass (but the real trajectory may not). This parameter provides a basis of characterizing supercircular entries irrespective of the atmosphere or the vehicle weight, shape, or size.

After the present research was well under way, a recent publication of Lees, Hartwig, and Cohen (ref. 1) became available in which they point out the pronounced alleviation of guidance requirements made possible by the application of aerodynamic lift and, in particular, by lift modulated in a certain fashion. They present results of numerical calculations for a specific vehicle entering the earth's atmosphere at a supercircular velocity of 35,000 feet per second, which provide a basis for comparison with the general results of the present analysis. Their discussion of entry with modulated lift stimulated the discussions herein of this type of entry.

NOTATION

a	resultant deceleration
A	reference area for drag and lift, sq ft
C_D	drag coefficient, $\frac{2D}{\rho V^2 A}$
C_q	coefficient the order of unity appearing in equation (A15)
C_Q	coefficient the order of unity appearing in equation (A16)
D	drag force, lb
F_p	perigee parameter $\frac{\rho_p \sqrt{r_p/\beta}}{2(m/C_D A)}$, dimensionless

g local gravitational acceleration

g_e earth sea-level gravitational acceleration, 32.2 ft sec^{-2}

G deceleration in earth sea-level g_e's, $\frac{a}{g_e}$

$\overline{G}$ dimensionless normalized deceleration (eq. (24))

l characteristic length of vehicle, ft

L lift force, lb

$\overline{L/D}$ average L/D during modulated-lift entry

m mass of vehicle, slugs

$\overline{M}$ molecular weight of atmosphere

Pr Prandtl number

q convective heating rate per unit area, Btu/sq ft sec

$\overline{q}$ dimensionless heating rate, $\overline{u}^{5/2}Z^{1/2}$ for laminar flow

Q total convective heat absorbed, Btu

$\overline{Q}$ dimensionless heat absorbed, $\int \overline{w}^{3/2}Z^{-1/2}d\overline{u}$ for shallow entries and laminar flow

r radius from planet center

r_o radius of planet

R radius of curvature of wall, ft, or universal gas constant

Re Reynolds number, $\frac{\rho V l}{\mu}$

s circumferential distance from conic perigee

S surface area wetted by boundary layer, sq ft

t time

T local temperature of ambient atmosphere

$\overline{T}$ mean temperature of planet atmosphere

u circumferential velocity component

$\overline{u}$ dimensionless ratio, $\frac{u}{\sqrt{gr}}$

V resultant velocity, $\frac{u}{\cos\gamma}$

$\overline{V}$ dimensionless ratio, $\frac{V}{\sqrt{gr}}$

y altitude, ft

Δy_p corridor width between conic perigee altitudes

$\Delta_{10}y$ altitude increment over which atmosphere density varies by factor of 10

Z dimensionless function of $\overline{u}$ determined from equation (3) and appropriate boundary conditions

α angle of attack of lifting surface relative to minimum-drag attitude

β atmospheric density decay parameter, ft^{-1}

γ flight-path angle relative to local horizontal; positive for climb

θ angle from planet center between conic perigee and vehicle position

μ coefficient of viscosity, slug ft^{-1}sec^{-1}

ρ atmosphere density, slug ft^{-3}

SUBSCRIPTS

ex exit from atmosphere

f final value

i initial value

0 surface of planet, or where $\overline{u}=0$

ov overshoot boundary

p conic perigee point

s stagnation point

un undershoot boundary

$\oplus$ relative to earth

SUPERSCRIPT

$'$ differentiation with respect to $\overline{u}$

ANALYSIS

OUTLINE OF APPROXIMATE ANALYTICAL METHOD AND FORMULAS FOR ENTRY MOTION AND HEATING

The approximate analytical method of reference 2 for studying entry motion is employed throughout this report. Details of the method are not described here; only an outline of the main equations is presented. In essence, the method is based on a single, nonlinear, differential equation (in dimensionless transformed variables) which represents the entry motion in an arbitrary planetary atmosphere. The full equation is given in appendix A with a list of associated formulas for various quantities relating to the motion and aerodynamic heating. Without obtaining any solution to this equation, but merely by examining its structure and its boundary conditions for the special case considered herein of shallow entries, we can establish three dimensionless parameters upon which entry motion and convective heating depend. One of the parameters involves the initial entry angle γ_i and arises because of mathematical convenience in specifying initial condi-

tions on the differential equation. In characterizing shallow supercircular entries—and especially in describing the guidance requirements for such entries—this initial-angle parameter is not as convenient as a different parameter which is subsequently introduced to replace the initial-angle parameter.

Basic differential equation.—Proceeding now with the mathematical outline, we select as an independent variable the dimensionless horizontal velocity referred to local values of g and of distance r from the plant center

$$\bar{u} \equiv \frac{u}{\sqrt{gr}} \tag{1}$$

and as a dependent variable the function

$$Z \equiv \frac{\rho \bar{u}}{2(m/C_D A)} \sqrt{\frac{r}{\beta}} \tag{2}$$

In this coordinate system the pair of motion equations for shallow entries ($\cos \gamma \cong 1$, $\overline{V} \cong \bar{u}$, $\sin \gamma \cong \gamma$) into a spherically symmetric planet reduced to a single, second order, nonlinear equation for the dimensionless Z function (ref. 2).

$$\underbrace{\bar{u} \frac{d^2 Z}{d\bar{u}^2}}_{\text{vertical acceleration}} - \underbrace{\left(\frac{dZ}{d\bar{u}} - \frac{Z}{\bar{u}}\right)}_{\text{vertical component of drag force}} = \underbrace{\frac{1-\bar{u}^2}{\bar{u}Z}}_{\text{gravity minus centrifugal force}} - \underbrace{\sqrt{\beta r} \frac{L}{D}}_{\text{lift force}} \tag{3}$$

The physical significance of the various terms is as indicated. It is to be noted that the molecular weight $\overline{M}$ and the local temperature T of the planet's atmosphere enter only in the parameter

$$\beta \equiv -\frac{1}{\rho} \frac{d\rho}{dy} = \frac{\overline{M} g}{\overline{R} T} \tag{4}$$

representing the local density gradient in the atmosphere: in any real atmosphere, β would vary moderately with altitude, and such variation is admissible within the framework of equation (3); equation (3) for $Z(\bar{u})$ is not restricted to exponential atmospheres, as we will see shortly. In the above form, though, it is restricted to small flight-path angles γ relative to the local horizontal (powers of $\cos \gamma$ appear on the right side of eq. (3) if γ is large as noted in appendix A), and to the condition $|(L/D) \tan \gamma| \ll 1$.

Inasmuch as the differential equation for $Z(\bar{u})$ is of second order, two initial conditions are required. The two conditions selected at the initial entry velocity $\bar{u}_i$ will, for the time being, be written as

$$Z(\bar{u}_i) = Z_i \qquad Z'(\bar{u}_i) = Z'_i \tag{5}$$

The dimensionless initial velocity, $\overline{V}_i = \bar{u}_i / \cos \gamma_i \cong u_i$, is employed to characterize the approach trajectory as being circular if $\overline{V}_i = 1$, elliptic if $1 < \overline{V}_i < \sqrt{2}$, parabolic if $\overline{V}_i = \sqrt{2}$, and hyperbolic if $\overline{V}_i > \sqrt{2}$. An entry is termed supercircular if $\overline{V}_i > 1$, and the local velocity is similarly termed if $\overline{V} > 1$. It is to be noted that the values of $m/C_D A$ and the initial altitude y_i are not needed in characterizing an entry motion by means of the Z function and its two initial conditions. After a Z function has been calculated, a number of quantities of engineering interest can readily be obtained from formulas listed in appendix A. Simple formulas relating aerodynamic heating and deceleration also are developed in this appendix and are shown to yield results for heating rates and total heat absorbed in good agreement with certain calculations for Earth entry presented by Lees, et al., in reference 1.

The characteristics of the planet's atmosphere enter the above equations mainly in the dimensionless parameter $\sqrt{\beta r}$. Approximate values of this parameter and other planetary constants used in numerical examples presented later are as follows (the subscript $\oplus$ designates a value relative to the earth):

PLANETARY CONSTANTS

	$r_\oplus$	$g_\oplus$	Gases	$\overline{M}$, gm/mol	$\overline{T}$, °K	$\sqrt{\beta r}$	$\sqrt{(\beta r)_\oplus}$	β^{-1}, ft	$\Delta_{10}y$ (for $\rho_2/\rho_1 = 10$), miles
Venus	0.97	0.87	CO_2, N_2	40	270	30	1.0	2×10^4	9
Earth	1.00	1.00	N_2, O_2	29	240	30	1.00	2.35×10^4	10
Mars	.53	.38	N_2, CO_2	28	200	14	.47	6×10^4	26
Jupiter	11.0	2.63	H_2, CH_4	3	170	60	2.0	6×10^4	26
Titan	.33	.22	CH_4	16	130	8	.27	10×10^4	43

The last two entries, Jupiter and Titan, are included in numerical examples presented later in order to illustrate the extreme variations encountered when entry into various atmospheres of the solar system is considered.

Computation of Z functions.—Inasmuch as the basic differential equation (3) for $Z(\overline{u})$ is nonlinear, it has been programed on an electronic computing machine (IBM 704) in order to obtain a large number of solutions for various values of the dimensionless parameters which determine an entry motion. Several hundred solutions were obtained for the results of this report. In order to start each solution, the first step from $\overline{u}_i$ to $\overline{u}_i-0.001$, was taken analytically. Over this small interval γ is essentially constant, so that the equations given in reference 2 for constant γ were applied to the first small step.

It may appear at first that little is gained over strictly numerical trajectory calculations as long as Z functions must also be computed on a machine. The gain, however, arises from increased generality of the results. One Z function can be applied to any planetary atmosphere and to a vehicle with any value of m/C_DA, whereas a conventional trajectory calculation would apply only to the specific atmosphere and specific value of m/C_DA employed.

Accuracy of Z function method.—The accuracy of the approximate analytical method may be judged from a comparison of several Z functions with more exact numerical calculations. If we first consider nonlifting vehicles, we see that with $L/D=0$ the basic differential equation (3) for Z would be independent of β and, hence, independent of any variations in atmosphere temperature with altitude as well as independent of m/C_DA. Exact calculations for a specific atmosphere and specific m/C_DA of the quantity $\rho\overline{u}\sqrt{r/\beta}/2(m/C_DA)$ provide a test of accuracy since this quantity as a function of $\overline{u}$ would coincide with $Z(\overline{u})$ if the approximate method were exact. Excellent agreement is exhibited in figure 1 between each of the two solid curves (one entry at $\overline{V}_i=1.25$, and one at $\overline{V}_i=1.4$) representing $Z(\overline{u})$ as computed from equation (3), and the corresponding points representing $\rho\overline{u}\sqrt{r/\beta}/2(m/C_DA)$ as computed from the pair of "exact" equations of motion with the same initial conditions. As noted in the figure, $Z(\overline{u})$ corresponds to arbitrary m/C_DA and an arbitrary atmosphere, while $\rho\overline{u}\sqrt{r/\beta}/2(m/C_DA)$ corresponds to $m/C_DA=1$ slug ft^{-2}, and to the ARDC (1956 model) atmosphere wherein the temperature varies in a prescribed manner with altitude. The latter calculations were obtained by use of the computing-machine program of Nielsen, Goodwin, and Mersman (ref. 3) applied to a spherically symmetric, nonrotating atmosphere. This close agreement for both entries exemplifies the accuracy of the approximate method and its applicability to nonexponential as well as exponential atmospheres.

If we now consider the case of a lifting vehicle, we see from the differential equation (3) that, *for a fixed L/D*, the Z function would not be independent of local variations in β with altitude, as is the case for $L/D=0$, since the parameter $\sqrt{\beta r}(L/D)$ would vary as $\sqrt{\beta r}$. An illustration of this may be seen from the small differences evident in figure 2 between the curve representing the Z function for constant $\sqrt{\beta r}(L/D)=32.5$ and the corresponding points representing the more exact calculations of $\rho\overline{u}\sqrt{r/\beta}/2(m/C_DA)$ for constant $L/D=1$, and $\sqrt{\beta r}(L/D)$ fluctuating with altitude (between values of about 28 and 33) according to the ARDC atmosphere. The small differences apparent in this particular case do not reflect an inaccuracy of the approximate Z function method, but merely exhibit the importance of atmospheric altitude-temperature variations for lifting vehicles. At the very lowest velocities ($\overline{u}<0.03$), though, the approximate theory breaks down because the approximation $|(L/D)\tan\gamma|<<1$ is no longer a good one.

PERIGEE PARAMETER FOR SPECIFYING AN ENTRY TRAJECTORY AND CORRIDOR WIDTH

Development of perigee parameter.—With confidence now in the accuracy of the approximate analytical method, we can examine the structure of the basic differential equation together with its boundary conditions in order to show that the initial parameter Z'_i can be replaced by one more convenient for characterizing shallow supercircular entries. From equation (A2) it follows that, for shallow entries starting at a high altitude where the initial values of ρ_i and hence Z_i are negligible compared to their corresponding values during entry, the second initial condition may be written as

$$Z'_i=\sqrt{\beta r}_i\,\gamma_i \tag{6}$$

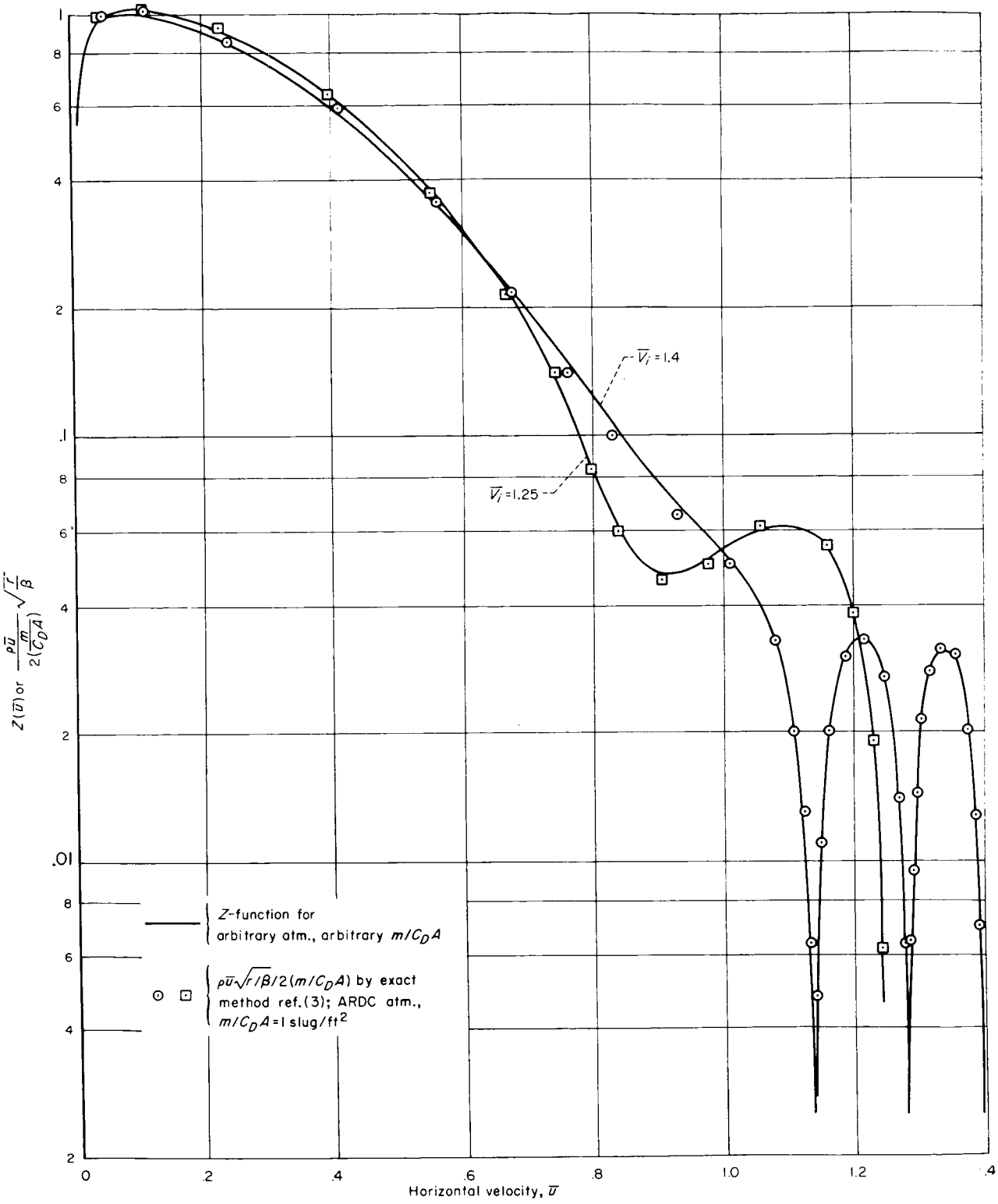

FIGURE 1.—Comparison of approximate Z function method with more exact calculations for nonlifting vehicles.

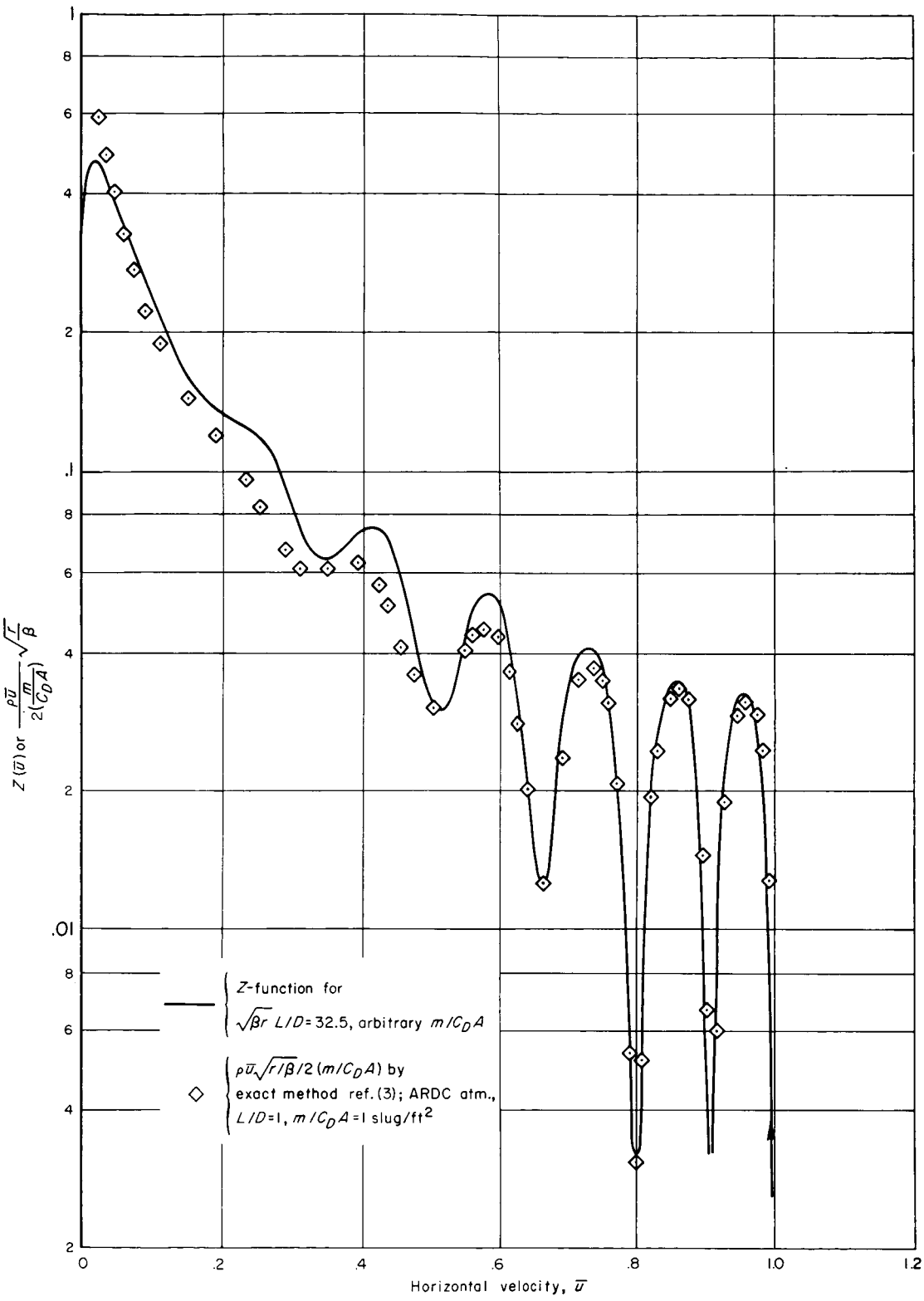

FIGURE 2.—Comparison of approximate Z function method with more exact calculations for a lifting vehicle.

532933—61——2

The initial flight-path angle γ_i should be taken at the beginning of the "sensible atmosphere." It is not a fully satisfactory parameter from a convenience standpoint because, for very shallow trajectories, such as grazing supercircular entries which just pass through an edge of atmosphere, the initial value of γ_i is cumbersome to define. Considerable supplementary information is required in order to state at just what altitude the sensible atmosphere begins for each particular vehicle; the appropriate altitude depends on m/C_DA, γ_i, and $\overline{u}_i$, as indicated in appendix B of reference 2.

The conic perigee point is not complicated as is the initial point for shallow entries; this may be illustrated with the help of figure 3. Shown in

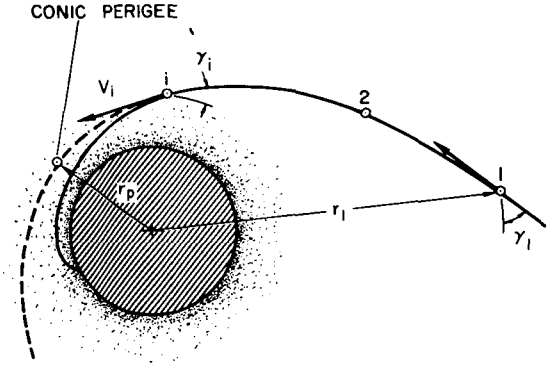

FIGURE 3.—Conic perigee.

the sketch is the hypothetical conic trajectory (short dashed line) which the vehicle would have followed had there been no atmosphere around the planet. This conic has a perigee of distance r_p from the planet center, but the actual trajectory may continuously descend and have no perigee. The entry trajectory could be specified equally well either through conditions at point (1) by the values of r_1, V_1, and γ_1, or at point (2) by an entirely different set of values r_2, V_2, and γ_2, or at the initial entry point (i) by a still different set r_i, V_i, and γ_i. All of these points, however, correspond to common values of radius r_p and velocity V_p at the conic perigee point where $\gamma_p=0$.

The value of r_p can be calculated readily from Newton's equations for a two-body drag-free trajectory

$$\frac{r_p}{r}=\frac{1-\sqrt{(\overline{V}^2-1)^2+\overline{V}^2(2-\overline{V}^2)\sin^2\gamma}}{2-\overline{V}^2} \tag{7}$$

where

$$\overline{V}\equiv\frac{V}{\sqrt{gr}}=\frac{\overline{u}}{\cos\gamma} \tag{8}$$

Since we are considering only shallow entries for which the flight-path angle is small, we employ an approximate form of equation (7), evaluated at the initial point (valid if $\sin^2\gamma_i\cong\gamma_i^2$ and $\overline{V}_i^2(2-\overline{V}_i^2)\sin^2\gamma_i/(\overline{V}_i^2-1)^2<<1$)

$$\frac{r_i-r_p}{r_i}\cong\frac{\overline{V}_i^2\gamma_i^2}{2(\overline{V}_i^2-1)} \tag{9}$$

The limitations resulting from this approximation are discussed later.

The initial condition imposed on the differential equation for the Z function can now be combined with the relationship (9) just derived to show the equivalence between $\sqrt{\beta r_i}\,\gamma_i$ and a certain perigee parameter defined in terms of conditions at the conic perigee (subscript p). We introduce a perigee parameter defined by

$$F_p\equiv\frac{\rho_p}{2(m/C_DA)}\sqrt{\frac{r_p}{\beta}} \tag{10}$$

For an atmosphere which is essentially exponential between the initial point and the conic perigee point, we have $\rho_p/\rho_i=e^{\beta(r_i-r_p)}$. From the definition of Z (eq. (2)) we also have $Z_i=\overline{u}_{i\rho i}\sqrt{r_i/\beta}/2(m/C_DA)$, so that

$$F_p=\frac{Z_i}{\overline{u}_i}\sqrt{\frac{r_p}{r_i}}\,e^{\beta(r_i-r_p)} \tag{11}$$

For shallow entries, γ_i^2 can be disregarded compared to unity, yielding $\overline{u}_i^2=\overline{V}_i^2\cos^2\gamma_i\cong\overline{V}_i^2$, while r_p/r_i in equation (11) can be set equal to unity consistent with the approximation made in writing equation (9). Thus, by combining (9) and (11),

$$F_p=\frac{Z_i}{\overline{V}_i}\,e^{\frac{\overline{V}_i^2(\sqrt{\beta r_i}\,\gamma_i)^2}{2(\overline{V}_i^2-1)}} \tag{12}$$

We see from this latter equation that for the case of shallow entries, $\sqrt{\beta r_i}\,\gamma_i$ is a function only of $\overline{V}_i$, Z_i, and F_p. Consequently, the two initial conditions, Z_i and $Z'_i=\sqrt{\beta r_i}\,\gamma_i$, imposed at $\overline{u}_i$ on the basic differential equation can, if desired, be replaced by the equivalent two, Z_i and F_p, imposed at $\overline{V}_i$ (for shallow entries $\overline{V}=\overline{u}$); in effect, then, F_p replaces $\sqrt{\beta r_i}\,\gamma_i$ as one of the two initial

conditions. Throughout the rest of this report the perigee parameter $F\rho$ is used as the basic parameter describing shallow supercircular entries, rather than $\sqrt{\beta r_i}\,\gamma_i$. Its use conveniently characterizes such entries because it is applicable to any planet, and to a vehicle of any m/C_DA. The value of F_p is easily calculated from two-body trajectory equations without concern for where the sensible atmosphere begins. It is noted that in the earth's atmosphere an increase in the perigee parameter F_p by a factor of 10, for example, means that the re-entry trajectory would be "aiming" at a conic perigee altitude about 10 miles lower, since the density changes by a factor of 10 in 10 miles (see table, p. 4, for $\Delta_{10}y$ of other planets).

Summarizing, we see that three dimensionless parameters determine shallow entry motion: the entry velocity $\overline{V}_i$, the lift parameter $\sqrt{\beta r}(L/D)$ which appears in the differential equation, and the perigee parameter F_p.

For later use, it is noted here that the angular distance s_0/r from the conic perigee to the point of impact ($\overline{u}=0$ as illustrated in fig. 4) can be shown

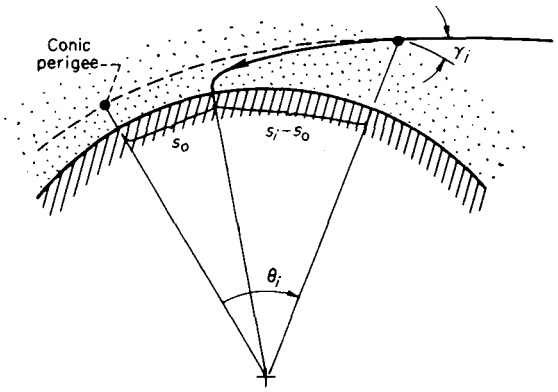

FIGURE 4.—Range notation.

to depend on only the same three parameters as Z depends on, $\overline{V}_i$, $\sqrt{\beta r}(L/D)$, and F_p. To this end we start with the defining equation,

$$\frac{s_0}{r}\equiv\theta_i-\frac{s_i-s_0}{r} \tag{13}$$

where θ_i is the angle between the conic perigee and the initial point. From equation (A5) for $(s-s_i)/r$, and the $\theta-\gamma$ relationship for two-body trajectories

$$\sin\theta=\frac{\overline{V}^2\sin 2\gamma}{2[\overline{u}^2(r/r_p)-1]} \tag{14}$$

which, for small angles becomes

$$\theta_i=\frac{\overline{V}_i^2\gamma_i}{\overline{V}_i^2-1} \tag{15}$$

at the initial conditions, we obtain the equation

$$\sqrt{\beta r}\,\frac{s_0}{r}=\frac{\overline{V}_i^2(\sqrt{\beta r_i}\,\gamma_i)}{\overline{V}_i^2-1}+\int_{\overline{u}_i}^{0}\frac{d\overline{u}}{Z} \tag{16}$$

Since all members on the right side of this latter equation depend only on $\overline{V}_i$, $\sqrt{\beta r}(L/D)$, and $\sqrt{\beta r}\,\gamma_i$ (or F_p), the quantity $\sqrt{\beta r}(s_0/r)$ is similarly dependent. This relationship is utilized later to specify the landing point of nonlifting vehicles entering at supercircular velocity.

Some remarks are in order here about the assumptions made in demonstrating the equivalence of F_p and $\sqrt{\beta r_i}\,\gamma_i$. The development is restricted to entries which are shallow ($\sin\gamma_i\cong\gamma_i$) and to entry velocities not too near circular in order that equation (9) be a good approximation. An examination of the higher order terms omitted from equation (9) reveals that this equation is not a good approximation if $\overline{V}_i^2-1<\gamma_i$, which corresponds to near-circular entries for which the angle θ_i between the Keplerian perigee and the initial point is greater than about 90°. Since γ_i is the order of 0.1 (or less) near $\overline{V}=1$ for most manned entries that are deceleration-limited, the use of F_p as a correlating parameter for similarity of entries into different planetary atmospheres is restricted to about $\overline{V}_i^2>1.1$ or $\overline{V}_i>1.05$. For the domain of planetary similarity in terms of F_p, namely, for shallow supercircular entries at $\overline{V}_i>1.05$, it would make no appreciable difference whether the full or the approximate equations were employed. The full equations are (7), (11), (14), the full differential equation (A1) for Z, and the associated equations which include cos γ factors. The corresponding approximate equations are (9), (12), (15), the approximate differential equation (3) for Z, and associated equations which use cos $\gamma=1$, sin $\gamma=\gamma$. For $\overline{V}_i<1.05$, however, it would make a difference whether full or approximate equations were employed. In making all numerical computations the full equations were used (with $\sqrt{\beta r}=30$), since these equations are only slightly more lengthy to program on an IBM 704 than are the corresponding approximate equations, but in presenting all results, they

are plotted in terms of the dimensionless parameters appropriate for planetary similarity. Consequently, in the range $1 \leq \overline{V}_i \leq 1.05$, the results plotted in subsequent figures, strictly speaking, would apply only to Earth ($\sqrt{\beta r}=30$), but in the range $\overline{V}_i > 1.05$ they would apply to any planet.

It is noted also that, in the development of equation (11) for F_p, the value of β tacitly has been assumed constant. Actually, β in equation (6) would properly be β_i and in equation (11), some mean value β_{mean} averaged between r_p and r_i. An improvement in accuracy can be obtained by regarding $\sqrt{\beta_r}$ in these equations as the "semi-local" value (see ref. 2) averaged over a small strip of altitude just above the conic perigee altitude, rather than by regarding it as equal to the average for the entire atmosphere ($\sqrt{\beta_r} \cong 30$ for Earth).

Definition of corridor width.—If we have two trajectories bounding an entry corridor, the difference $\Delta y_p \equiv y_{p_{ov}} - y_{p_{un}}$ between their two conic perigee altitudes is defined as the corridor width, as illustrated in figure 5. By employing the exponential-atmosphere approximation between $y_{p_{ov}}$ and $y_{p_{un}}$ there results, from the defining equation (10) for the perigee parameter,

$$\Delta y_p \equiv y_{p_{ov}} - y_{p_{un}} = \frac{1}{\beta} ln \frac{(F_p m/C_D A)_{un}}{(F_p m/C_D A)_{ov}} \tag{17}$$

or, in terms of the altitude increment $\Delta_{10} y$ over which atmospheric density changes by a factor of 10,

$$\Delta y_p = \Delta_{10} y \log_{10} \frac{(F_p m/C_D A)_{un}}{(F_p m/C_D A)_{ov}} \tag{18}$$

For the special case wherein $m/C_D A$ is the same along the two boundaries,

$$\Delta y_p = \Delta_{10} y (\log_{10} F_{p_{un}} - \log_{10} F_{p_{ov}}) \tag{19}$$

It is to be noted from equation (18) that, in a given exponential atmosphere (constant β), the corridor width for any fixed $m/C_D A$ depends only on $F_{p_{un}}/F_{p_{ov}}$, and is independent of $m/C_D A$. The altitude of a corridor boundary, or of the corridor center, however, depends on $m/C_D A$ since $\rho_p \sim m/C_D A$ (see eq. (10)). In the earth's atmosphere the corridor width would vary a small amount (about ± 10 percent) because of the variation of β with altitude, latitude, and season.

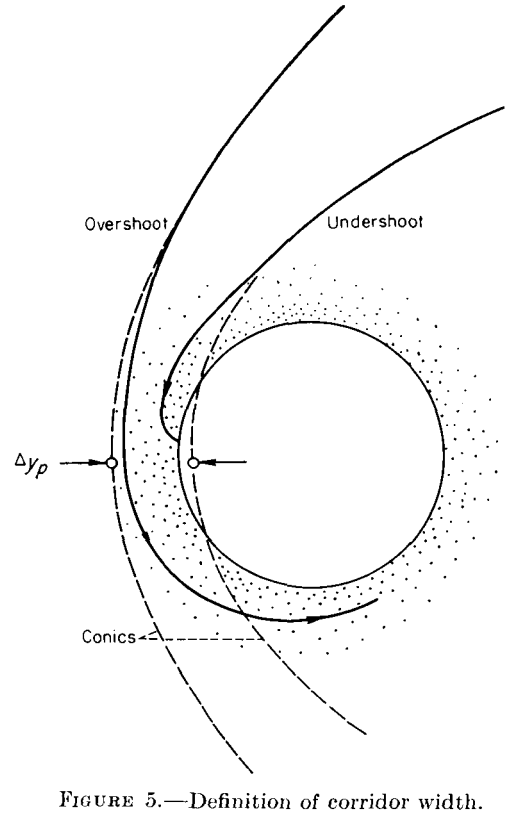

FIGURE 5.—Definition of corridor width.

DETERMINATION OF GUIDANCE REQUIREMENTS FROM CORRIDOR WIDTH

Since the width of the entry corridor between the conic perigee altitudes of overshoot and undershoot is independent of $m/C_D A$, it provides a convenient basis for calculating and visualizing guidance requirements. From a knowledge of the corridor width $\Delta y_p = y_{p_{ov}} - y_{p_{un}}$ between conic perigees, the corresponding guidance requirements on velocity and flight-path angle can be calculated from equation (7) representing a conic trajectory in terms of $\overline{V}$ and γ:

$$\frac{r_p}{r} = f(\overline{V}, \gamma) \equiv \frac{1 - \sqrt{1 - \overline{V}^2(2 - \overline{V}^2)\cos^2\gamma}}{2 - \overline{V}^2} \tag{20}$$

$$= \frac{\overline{V}^2 \cos^2\gamma}{1 + \sqrt{1 - \overline{V}^2(2 - V^2)\cos^2\gamma}}$$

If the corridor width is relatively narrow, the errors, $\Delta\overline{V}$, $\Delta\gamma$, and Δr at any given distance r from the planet are related to the change in conic

perigee altitude $\Delta y_p = \Delta r_p$ which they produce through the derivatives of the above function.

$$\frac{\Delta r_p}{r} = \frac{\partial f}{\partial \overline{V}} \Delta \overline{V} + \frac{\partial f}{\partial \gamma} \Delta\gamma + \frac{f}{r} \Delta r \tag{21}$$

These derivatives become especially simple for the case of parabolic entry ($\overline{V}^2 = 2$ and $2r_p = r\overline{V}^2 \cos^2\gamma$).

$$\left(\frac{\Delta y_p}{r_p}\right)_{\overline{V}=\sqrt{2}} = 2\frac{\Delta \overline{V}}{\overline{V}} - 2\sqrt{\frac{r}{r_p}\left[1-\left(\frac{r_p}{r}\right)\right]}\Delta\gamma + \frac{\Delta r}{r} \tag{22}$$

For narrow corridors $r_p \cong r_0$, so that the permissible velocity error $\Delta\overline{V}/\overline{V}$ for zero error in γ and r is simply $\Delta r_p/2r_0$, independent of r. The permissible $\Delta\gamma$ error for zero errors in r and $\overline{V}$, however, would decrease substantially as r increases. Some examples of the calculated guidance requirements for entering the corridors of various planets are presented later in terms of the plus-or-minus tolerances about the corridor center-line trajectory (e.g., $\pm\Delta\gamma = \Delta\gamma/2$). It may suffice as a reference point to note here that a 10-mile wide corridor in the earth's atmosphere ($\Delta y_p/r_0 = 1/400$) would require, at a distance of 10 earth radii, a flight-path angle accuracy of about $\pm\Delta\gamma = 0.01°$ if there were no errors in velocity or position.

RESULTS AND DISCUSSION

In what follows the simplest case of nonlifting entry is discussed first, with attention being given to the corridor boundaries, corridor width, and aerodynamic heating problems. Lifting entry is then discussed giving consideration to the interdependence of C_D and L/D, inasmuch as such consideration is necessary in realistically evaluating the net broadening of the entry corridor made possible through the use of lift, as well as in evaluating the aerodynamic heating penalty associated with lifting vehicles. In the final section, a brief discussion is presented of the guidance tolerances imposed by the corridor widths for supercircular entry into various planets.

In the presentation of many results which follow a normalization technique is used. Thus equation (A4) for the resultant deceleration in earth g's for shallow entry

$$\overline{G} \equiv \frac{a}{g_e} = g_\oplus \sqrt{\beta r}\, \bar{u} Z \sqrt{1+\left(\frac{L}{D}\right)^2} \tag{23}$$

is normalized with respect to the earth by a dimensionless function $\overline{G}$ defined by

$$\overline{G} \equiv 30\, \bar{u} Z \sqrt{1+\left[\sqrt{(\beta r)_\oplus}\,\frac{L}{D}\right]^2} \tag{24}$$

where $\sqrt{(\beta r)_\oplus} \equiv \sqrt{\beta r}/30$. The normalized $\overline{G}$ function, like the Z function, depends only on the parameters $\sqrt{\beta r}(L/D)$, $\overline{V}_i$, and F_p, and is applicable to any planet. For the earth, $\overline{G}$ is equal to $30\, \bar{u} Z \sqrt{1+(L/D)^2}$, the deceleration in earth sea-level g's (see eq. (23)). For other planets, the deceleration G in earth g's can readily be obtained from $\overline{G}$ and the planetary constants by combining the above two equations.

$$G = g_\oplus \sqrt{(\beta r)_\oplus}\, \overline{G}\, \frac{\sqrt{1+(L/D)^2}}{\sqrt{1+[\sqrt{(\beta r)_\oplus} L/D]^2}} \tag{25}$$

The normalized distance from the conic perigee to the landing point is $\sqrt{(\beta r)_\oplus}(s_0/r)$, which is equal to s_0/r for the earth, and which also depends only on the same three parameters that Z depends upon. The dimensionless quantities $\overline{q}$ and $\overline{Q}$ (defined in appendix A) pertaining to convective heating in a planetary atmosphere are not normalized with respect to Earth.

SINGLE-PASS ENTRY OF NONLIFTING VEHICLES

The simple case $L/D = 0$ will serve to illustrate the generality of the perigee parameter, and its convenience in describing corridor boundaries. A plot of the maximum value of the normalized deceleration ($\overline{G}_{max}$) versus F_p is presented in figure 6 for various supercircular entry velocities. As indicated on the ordinate scale, $\overline{G}$ is equal to $G/g_\oplus\sqrt{(\beta r)_\oplus}$ for nonlifting vehicles (see eq. (25)). The circle points in this figure designate the overshoot boundary for single-pass entries. Thus, in a parabolic entry at essentially escape velocity ($\overline{V}_i = 1.4$), the overshoot boundary occurs at a perigee parameter of 0.06. If a parabolic approach trajectory aims at $F_p < 0.06$ (at a higher perigee having lower density and, hence, smaller F_p) the vehicle will pass through the atmosphere, orbit, and then return for at least a second pass before entry is completed; but, if the vehicle aims at $F_p > 0.06$, entry will be completed on the first pass. It is to be noted that the overshoot boundaries in terms of F_p apply to any planet.

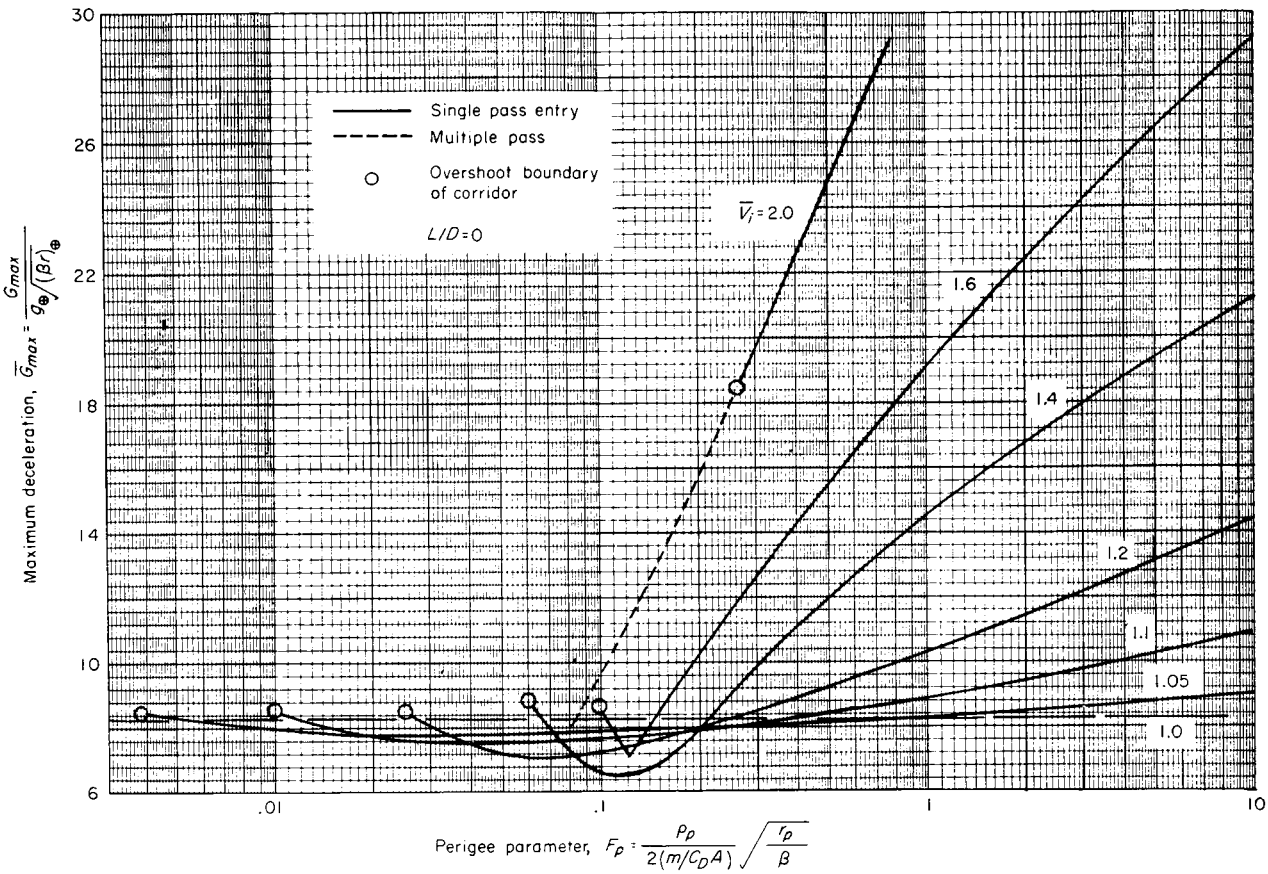

FIGURE 6.—Maximum deceleration during entry of nonlifting vehicles.

Undershoot boundaries and corridor widths can also be obtained readily from the normalized deceleration curves in figure 6 having $\log_{10}F_p$ as the abscissa. If m/C_DA is the same at overshoot and undershoot, the corridor width on such a plot is simply proportional to the spacing between the two abscissa points representing these boundaries (see eq. (19)). We will consider first the case of entry into Earth. If, for example, maximum deceleration is arbitrarily set at 10 G (ten times the earth's sea-level acceleration), the undershoot boundary for the earth would be at $\overline{G}_{max}=10$ in figure 6, and at $F_{p_{un}}=0.31$ for parabolic entry. The ratio $F_{p_{un}}/F_{p_{ov}}=0.31/0.06=5.1$, corresponds to 0.7 of a $\log_{10}$ cycle. Since one $\log_{10}$ cycle in F_p represents a corridor width equal to $\Delta_{10}y$ for a fixed m/C_DA (see eq. (19)), the width of the entry corridor between conic perigees in the present example is $0.7\Delta_{10}y$, which amounts to 7 miles for the earth. This corridor width would be the same for any fixed value of m/C_DA. If m/C_DA were increased by a factor of 100, however, both corridor boundaries (which correspond to fixed values of F_p) would be situated lower in altitude where the density is 100 times greater (20 miles lower for the earth), but the corridor width between the two boundaries would still be 7 miles for single-pass parabolic entries limited by 10 G deceleration. It is clear that by specifying the corridor width in terms of the width between conic perigees, it is a simple matter to compute the conventional plus-or-minus guidance tolerances at any distance from a planet from the well-known equations for two-body trajectories. Examples of this are presented later.

Turning now to different objects in the solar system, the entry corridor widths can be shown to vary over wide limits, as might be anticipated. The example value $\overline{G}_{max}=10$ of normalized deceleration would correspond in the case of Jupiter, for instance, to a deceleration of 53 Earth g's, since $g_\oplus\sqrt{(\beta r)_\oplus}$ is 5.3 for Jupiter (see eq. (25)). Since one $\log_{10}$ cycle in F_p corresponds to 26 miles altitude on Jupiter (see table, p. 8, of planetary

constants), this 53 G_{max} corridor width for parabolic entry would be $0.7\times26=18$ miles. The 10 G_{max} corridor width would be nonexistent, since the smallest possible maximum deceleration for nonlifting vehicles entering any planet corresponds to $\overline{G}_{max}=6.5$ (this may be seen from fig. 6 or, more clearly, from a cross plot presented later), which corresponds to $6.5\times5.3=34$ G for Jupiter. On the other extreme, this example value $\overline{G}_{max}=10$ in the case of Titan ($g_{\oplus}\sqrt{(\beta r)_{\oplus}}=0.06$) would correspond to a maximum deceleration of only 0.6 G, and to a corridor width of $0.7\times43=30$ miles for this small value of maximum deceleration. Since even normal entry at parabolic velocity would result in only 5.2 G for Titan, the corridor width for 10 G_{max} would actually be the full radius of Titan (1300 miles) plus the conic perigee altitude for overshoot (between about 50 and 250 miles, depending on m/C_DA and the surface-level atmosphere density on Titan). Similar calculations yield the following table of corridor widths for nonlifting vehicles entering at parabolic velocity (a value of 0 for the corridor width designates nonexistence of a corridor in the sense that the minimum possible G_{max} is less than the value arbitrarily selected for the undershoot boundary)

	Corridor width in miles for $L/D=0$, $\overline{V}_i=1.4$			
	5 G_{max}	10 G_{max}	20 G_{max}	40 G_{max}
Venus	0	8	23	80
Earth	0	7	20	70
Mars	210	400	1250	2200
Jupiter	0	0	0	10
Titan	1300	1400	1400	1400

An approximate increment of 100 miles for the overshoot altitude has been included in the estimates for Titan. For Mars an increment of 80 miles has been included (corresponding to $L/D=0$, $m/C_DA=1$ slug/sq ft, and to a surface-level atmosphere density of 0.0002 slug/cu ft).

An interesting, and possibly unexpected, result for the entry of nonlifting vehicles is exhibited by

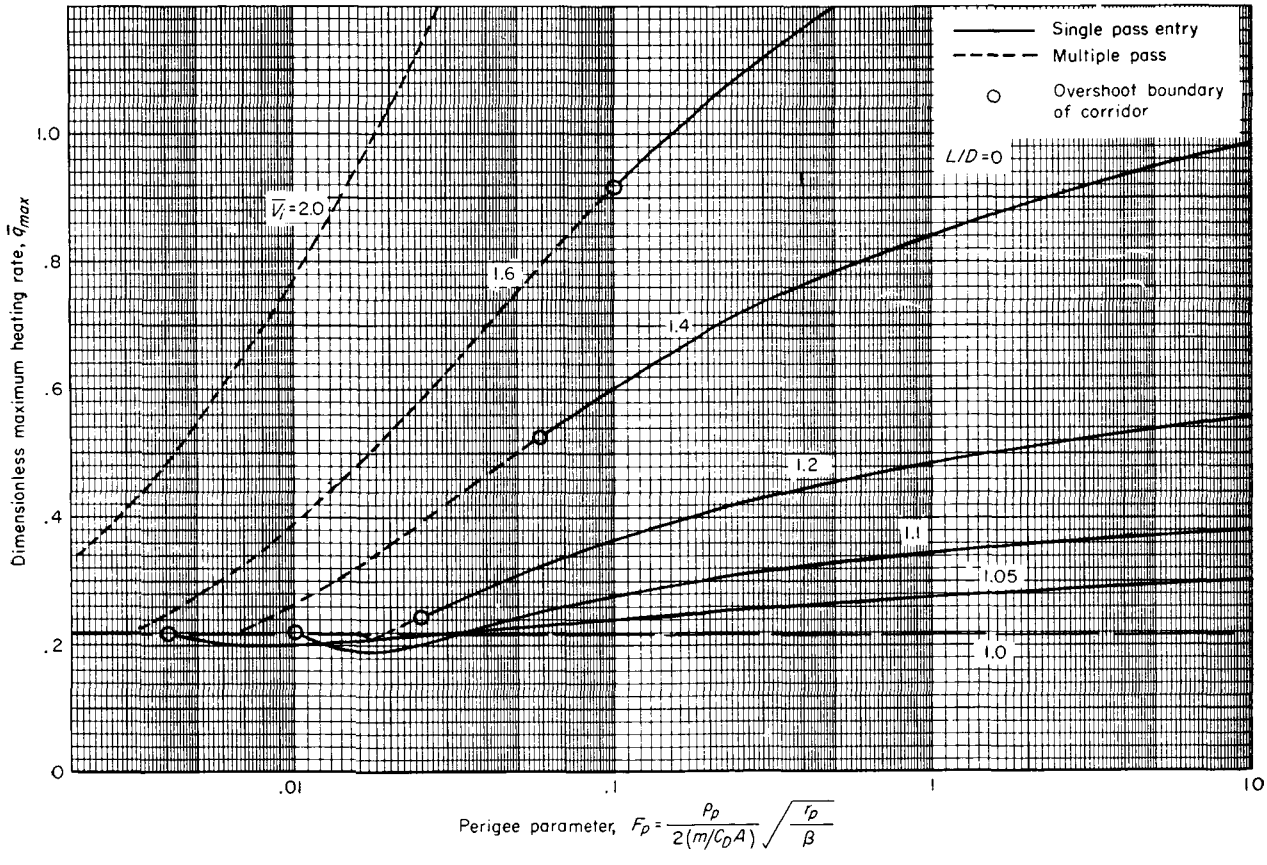

FIGURE 7.—Maximum laminar heating rate during entry of nonlifting vehicles.

the curves for maximum deceleration in figure 6, and also by the curves for maximum rate of laminar heating in figure 7. The minimum values of $\bar{G}_{max}$ and $\bar{q}_{max}$ do not occur at the lowest supercircular entry velocity (circular velocity, $\bar{V}_t=1$), as might be expected on first thought. These minima occur for entry velocities that are substantially supercircular. This is apparent from a cross plot of the various minima, as presented in figure 8.

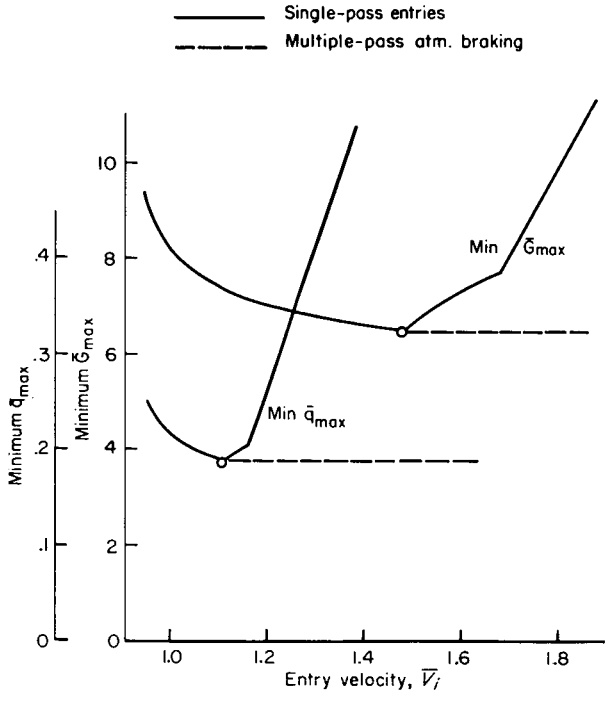

FIGURE 8.—Cross plot of the minimum values of the maximum deceleration and maximum heating rate as a function of entry velocity for nonlifting vehicles.

The least possible maximum deceleration would be experienced by entering a planet at a hyperbolic velocity of $\bar{V}_t=1.48$ and aiming at a perigee parameter of $F_p=0.12$, resulting in $\bar{G}_{max}=6.5$ (as compared to $\bar{G}_{max}=8.3$ for circular orbital decay). The least possible maximum heating rate for nonlifting vehicles occurs at $\bar{V}_t=1.12$ and at $F_p=0.018$, resulting in $\bar{q}_{max}=0.19$ as compared to $\bar{q}_{max}=0.22$ for circular orbital decay.

The physical reason these minima occur at supercircular rather than at circular entry velocity is that supercircular velocity is accompanied by a greater centrifugal lifting force than circular velocity, and, hence, results beneficially in slower rates of descent. If $\bar{V}_t$ is not too much greater than unity, this beneficial effect of centrifugal lift dominates over the detrimental effect of increased velocity, whereas for very large $\bar{V}_t$ the latter effect dominates. The net result is a minimum at some supercircular $\bar{V}_t>1$. In different terms, these minima arise at $\bar{V}_t>1$ rather than at $\bar{V}_t=1$ because, by the time the local velocity for entry at $\bar{V}_t>1$ has been reduced to $\bar{V}=1$, the vehicle is in essentially level flight (not necessarily in a slight climb) at an altitude where the deceleration is sizable; as a result, by the time the vehicle descends to the relatively lower altitudes at which G_{max} or q_{max} would be experienced if $\bar{V}_t$ were unity, the velocity has been reduced relatively much more. Thus in supercircular entry, the maximum conditions are experienced at higher altitudes where they are less severe than in circular entry.

The normalized curves for the total heat absorbed during nonlifting entry are presented in figure 9. They do not exhibit minima. For any entry velocity the least possible total heat is absorbed by entering at the largest possible value of F_p, corresponding to the steepest possible descent and to the greatest possible deceleration. This result is to be anticipated from the general inverse relationship between $\bar{Q}$ and deceleration previously developed as equation (A14), and would apply also for lifting vehicles. Near the overshoot boundary, where the decelerations are the smallest, $\bar{Q}$ is the largest. For parabolic entry $\bar{Q}=4.3$ at the overshoot boundary ($F_{p_{ov}}=0.06$), whereas at the $\bar{G}_{max}=10$ undershoot boundary ($F_{p_{un}}=0.31$) the corresponding value $\bar{Q}=2.1$ is half that at overshoot. As will be seen later, the difference between $\bar{Q}$ at the two boundaries for lifting vehicles can be considerably greater.

Normalized curves giving the landing point relative to the conic perigee point are presented in figure 10. As would be expected, the point of impact for vehicles aiming at a given F_p moves around the planet in the direction of motion (from positive toward negative s_0) as the entry velocity is increased. Except for entries near the overshoot boundaries, though, the landing point is surprisingly near the conic perigee point and is not greatly affected by $\bar{V}_t$. Thus, in the range $1\leq F_p\leq 10$, a nonlifting vehicle would impact before the vehicle passes under the conic perigee point, always landing within a distance of about $0.25r$ of the conic perigee for any $\bar{V}_t$ between 1.05 and 2.0.

The various charts presented for nonlifting vehicles cover only the range of shallow entries for

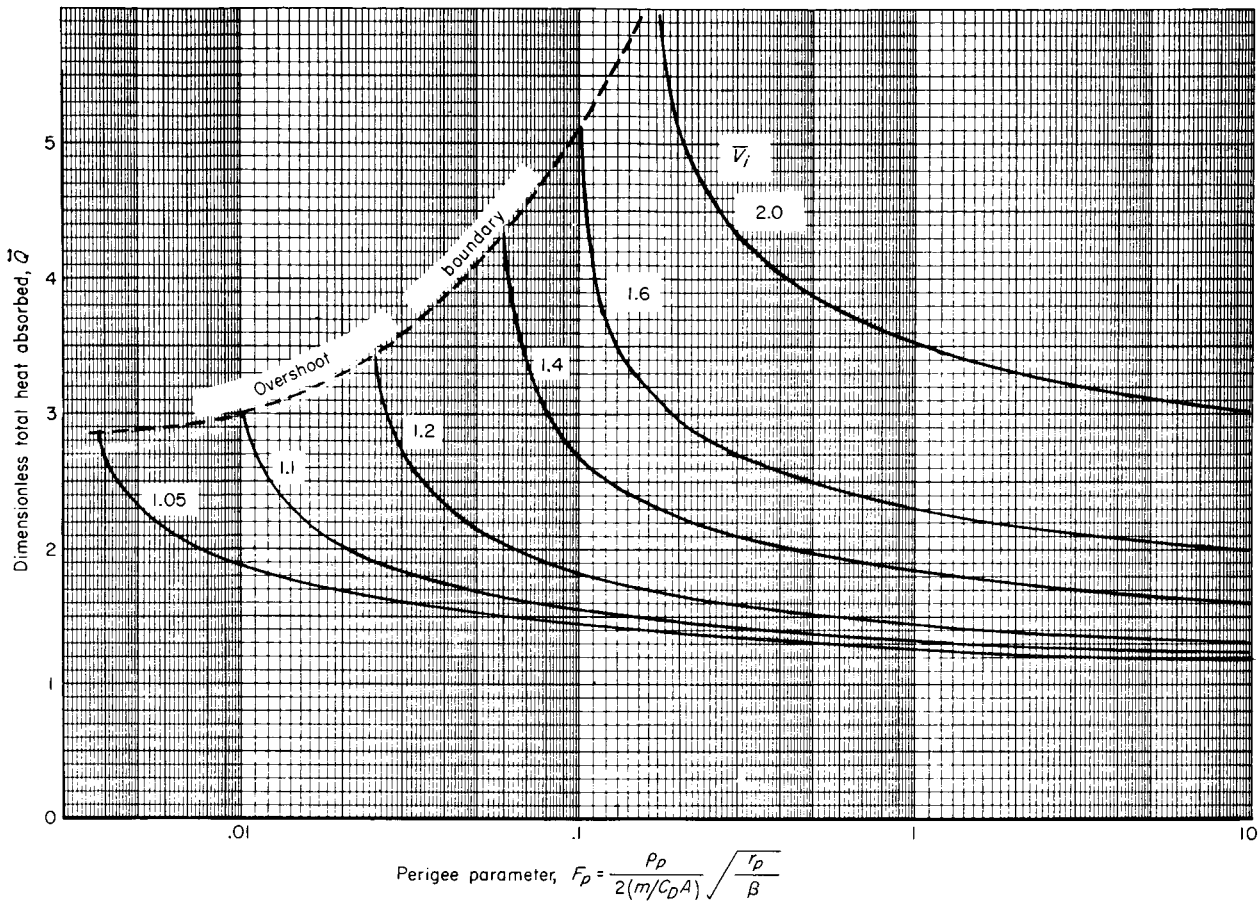

FIGURE 9.—Total laminar heat absorbed during entry for nonlifting vehicles.

$F_p \leq 10$. Beyond this value the entries become so steep that the gravity and centrifugal forces are small compared to the vertical components of drag and deceleration. Under such circumstances the solution of Allen and Eggers (ref. 4) for a constant flight-path angle would apply. It is shown in reference 2 that this particular solution corresponds to a function Z_I given by

$$Z_I = \sqrt{\beta r} \sin \gamma_i \bar{u} \ln \frac{\bar{u}}{\bar{u}_i} \tag{26}$$

and to

$$G_{max} = \frac{g_\oplus \beta r (-\sin \gamma_i)}{2e} \bar{V}_i^2 \tag{27}$$

$$\bar{q}_{I_{max}} = 0.247 \bar{u}_i^3 (-\sqrt{\beta r} \sin \gamma_i)^{1/2} \tag{28}$$

$$\bar{Q}_I = \bar{V}_i^2 \frac{\sqrt{\pi/2}}{(-\sqrt{\beta r} \sin \gamma_i)^{1/2}} \tag{29}$$

These equations can be used for the steeper entries. The use of γ_i for steep entries is not arbitrary, and is probably more convenient than the use of F_p. The conic perigee radius of a steep entry, if desired, is readily calculated from equation (7), the corridor width would be simply $r_0 - r_p$, and the landing point would be at an angle θ_0 from perigee, where θ_0 is calculated from the full equation (14) for θ.

OVERSHOOT BOUNDARY FOR LIFTING VEHICLES

Before discussing the influence of aerodynamic lift on the corridor boundaries it is desirable to note that such discussion considers the interrelationship between L/D and C_D. Any coupling between L/D and C_D takes on added significance when aerodynamic heating is considered, since corridor width and aerodynamic heating each depends on both L/D and C_D, and in conflicting ways. It is unfortunate that shapes cannot be designed to have maximum L/D with simultaneously maximum C_D. Large C_D is desirable in order to minimize aerodynamic heating (see ref. 4, or eqs. (A13) and (A14)), and large L/D is desir-

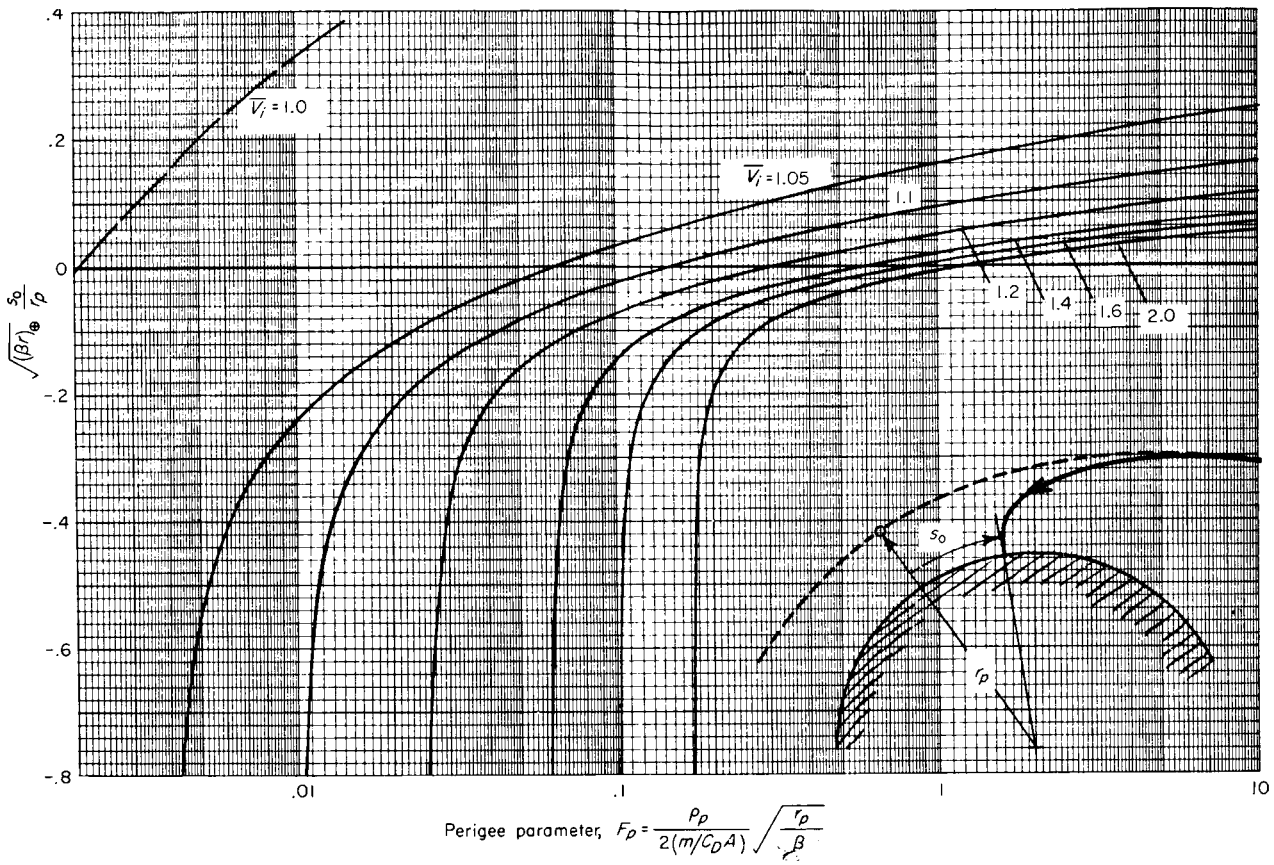

FIGURE 10.—Horizontal distance from conic perigee to landing point of nonlifting vehicles.

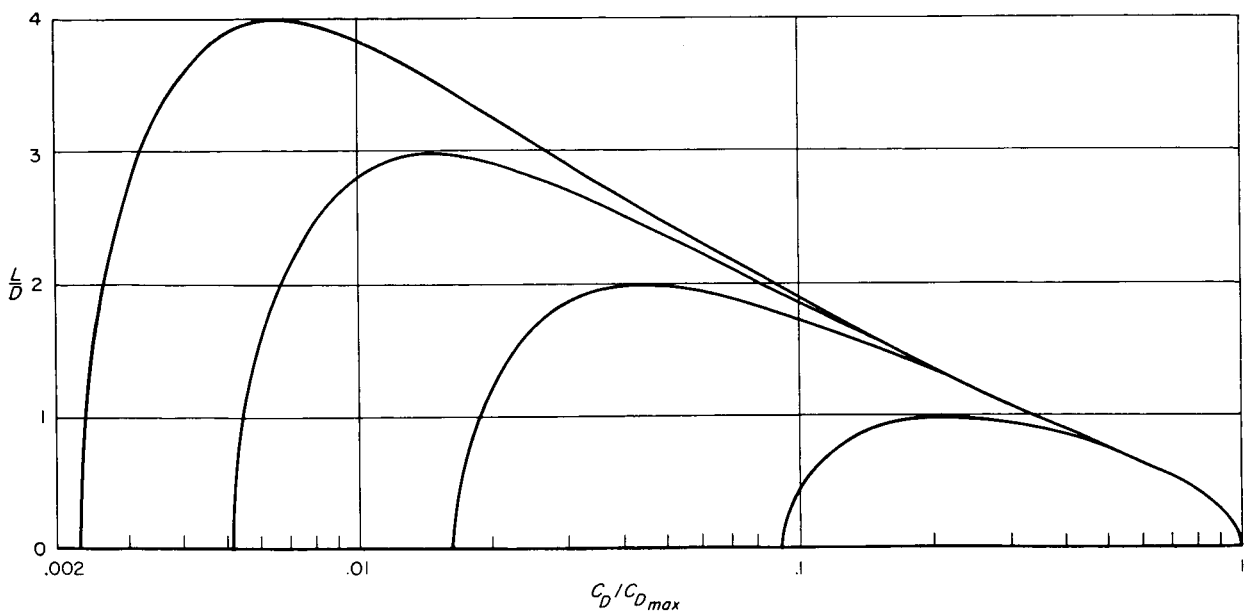

FIGURE 11.—Lift-drag polars for lifting surfaces in hypersonic Newtonian flow.

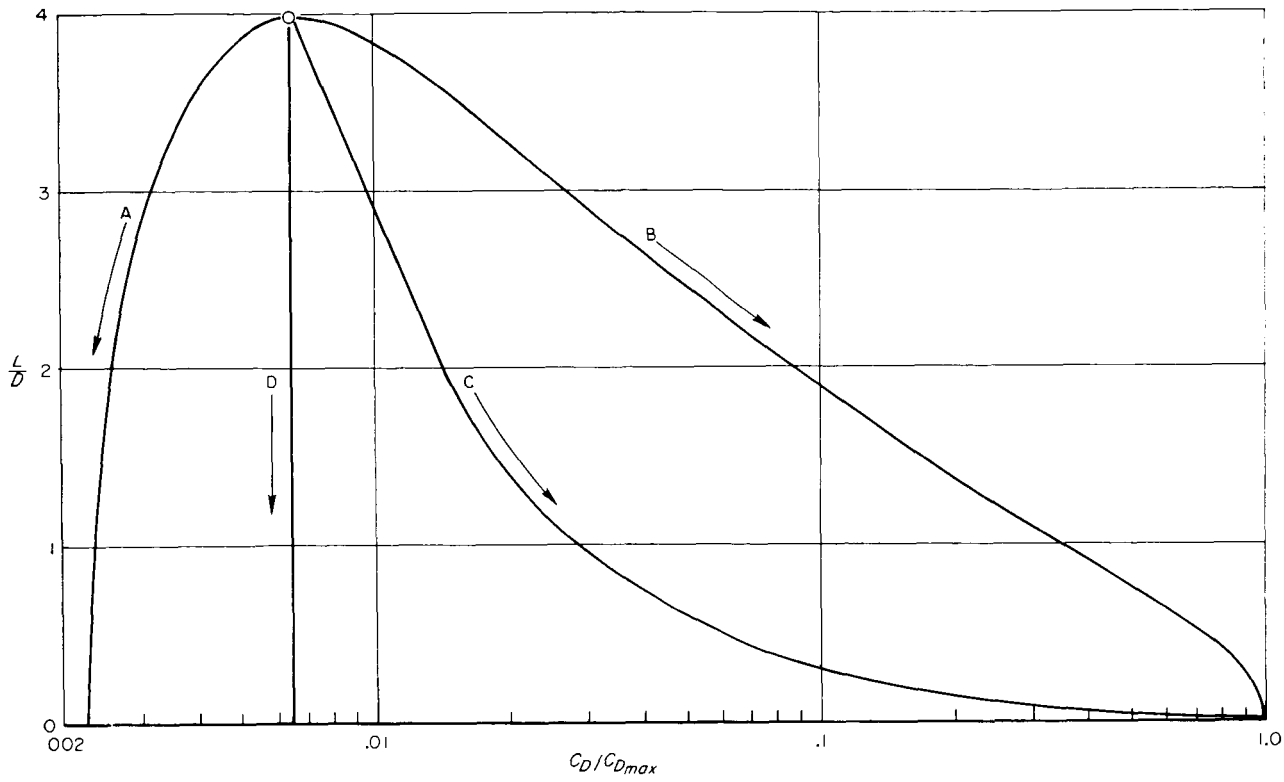

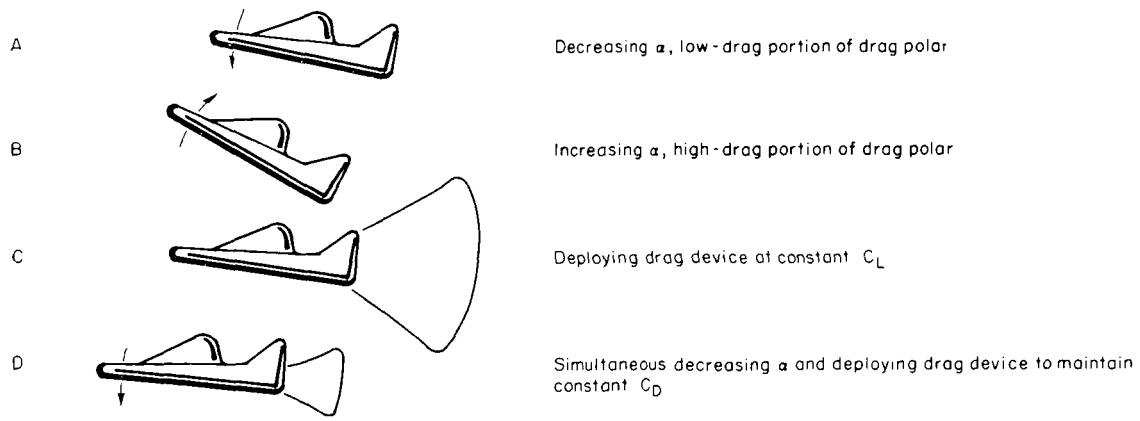

FIGURE 12.—Interdependence of C_D and L/D for four different methods of varying L/D between 4 and 0.

able in order to maximize the corridor width. High L/D values are obtained, however, only with slender shapes having low C_D, whereas low L/D values can be obtained either with large C_D (blunt shapes, or slender shapes at large angle of attack α) or with small C_D (slender shapes at small α). The approximate dependence of L/D on C_D for lifting surfaces in hypersonic Newtonian flow is developed in appendix B, and is illustrated by the four curves in figure 11. As noted in this appendix, the C_D-L/D coupling represented by the top curve in figure 11 produces the largest C_D for a given L/D of the several cases considered (as illustrated by the curves in fig. 12), and, hence, is employed herein to evaluate the net broadening in corridor width which can be realized by employing

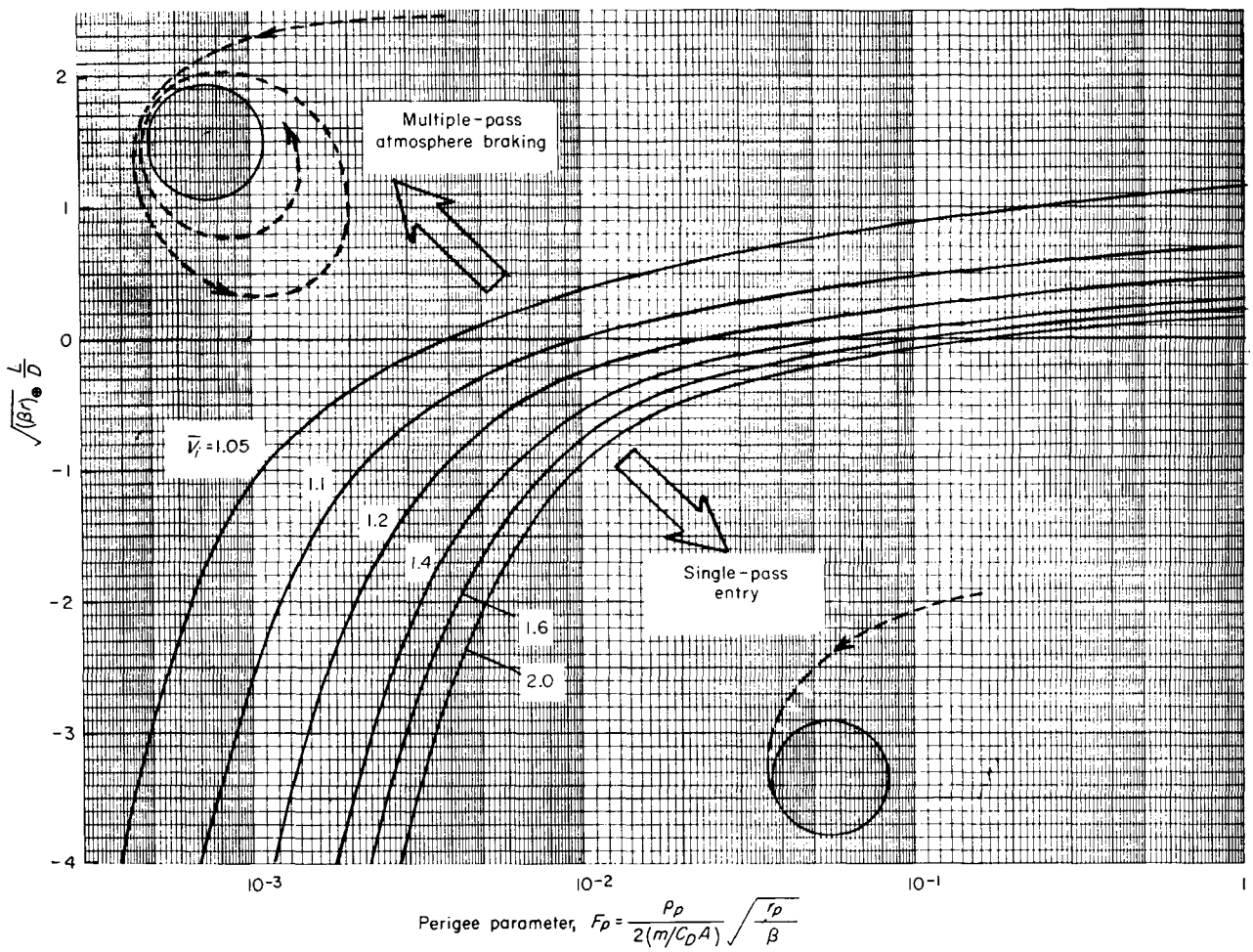

FIGURE 13.—Overshoot boundaries for single pass entries.

a lifting vehicle. This particular coupling also is employed to help evaluate the trade-off between guidance and heating problems.

Determination of overshoot boundary.—If a vehicle entered along the overshoot boundary, it would pass through barely enough atmosphere to just reduce the velocity to local circular as the vehicle is about to exit from the atmosphere. The overshoot boundary has been determined by plotting a curve of the exit velocity $\overline{V}_{ex}$ for atmosphere braking passes as a function of F_p, and then observing the intercept at $\overline{V}_{ex}=1$. The results are presented in figure 13 in terms of the parameter $\sqrt{(\beta r)_\oplus}(L/D)$ (equal to L/D for Earth). Since each curve corresponds to $\overline{V}_{ex}=1$, the domain above and to the left of each curve represents multiple-pass atmosphere braking, whereas the domain below and to the right represents single-pass entry. These curves apply to any planet.

As might have been anticipated, the curves in figure 13 show that, relative to the case of $L/D=0$, the overshoot boundary can be extended upward (to lower ρ_p and lower F_p) if negative lift is employed, that is, lift directed toward the planet center. When the interdependence of L/D and C_D is considered, the actual extension in the conic perigee atlitude for overshoot ($\Delta y_{p_{ov}}$ is proportional to $\Delta \log F_{p_{ov}}/C_D$), would be less than the apparent extension in F_p because C_D decreases as L/D increases. Even the extension in F_p is not impressively large, and is of diminishing magnitude as L/D decreases, because the higher the vehicle passes, the less mass of atmosphere there is to deflect the trajectory toward the planet center. For Earth ($\sqrt{(\beta r)_\oplus}=1$) the curves plotted in figure 13 and the values

tabulated in appendix B for the C_D-L/D relationship yield the following results for the parabolic ($\overline{V}_i=1.4$) overshoot boundary expressed in terms of the increase $\Delta y_{p_{ov}}$ in the conic perigee altitude at overshoot.

L/D	Extension upward of $y_{p_{ov}}$ assuming constant C_D, miles	Extension upward of $y_{p_{ov}}$ considering C_D-L/D dependence, miles
0	0	0
−. 25	5	4. 8
−. 5	7. 5	6
−1	10	5
−2	12. 5	2
−4	15	−7

It is seen that when C_D-L/D coupling is considered, the highest conic perigee altitude for overshoot would be obtained with $L/D\cong-0.5$ and would be only 6 miles higher than that for $L/D=0$. The overshoot altitude for $L/D=-4$ actually is substantially lower than for $L/D=0$, illustrating that too much negative L/D at overshoot would result in a narrower corridor than if L/D were 0.

A more effective method of extending the overshoot boundary would be to deploy a large, light, high-drag device. In this way it appears practical to increase C_DA by a factor of about 1000. The corresponding conic perigee altitude at overshoot would be raised by an amount $3\ \Delta_{10}y$ (see eq. (18)), which is equal to 30 miles for Earth. This is 5 times the extension in overshoot attainable by the use of negative lift.

In addition to specifying the overshoot boundary ($\overline{V}_{ex}=1$), it also is of interest for hyperbolic entries to specify the nonreturn boundary ($\overline{V}_{ex}=\sqrt{2}$). Both boundaries are illustrated in figure 14 for $\overline{V}_i=1.6$ and $\overline{V}_i=2.0$. It is evident from the less than pencil-line width between solid and dashed curves that there is negligible difference between these boundaries in the range of $\sqrt{(\beta r)_\oplus}$ (L/D) less than about −0.5. Even for $L/D=0$ there is little difference, the overshoot boundary

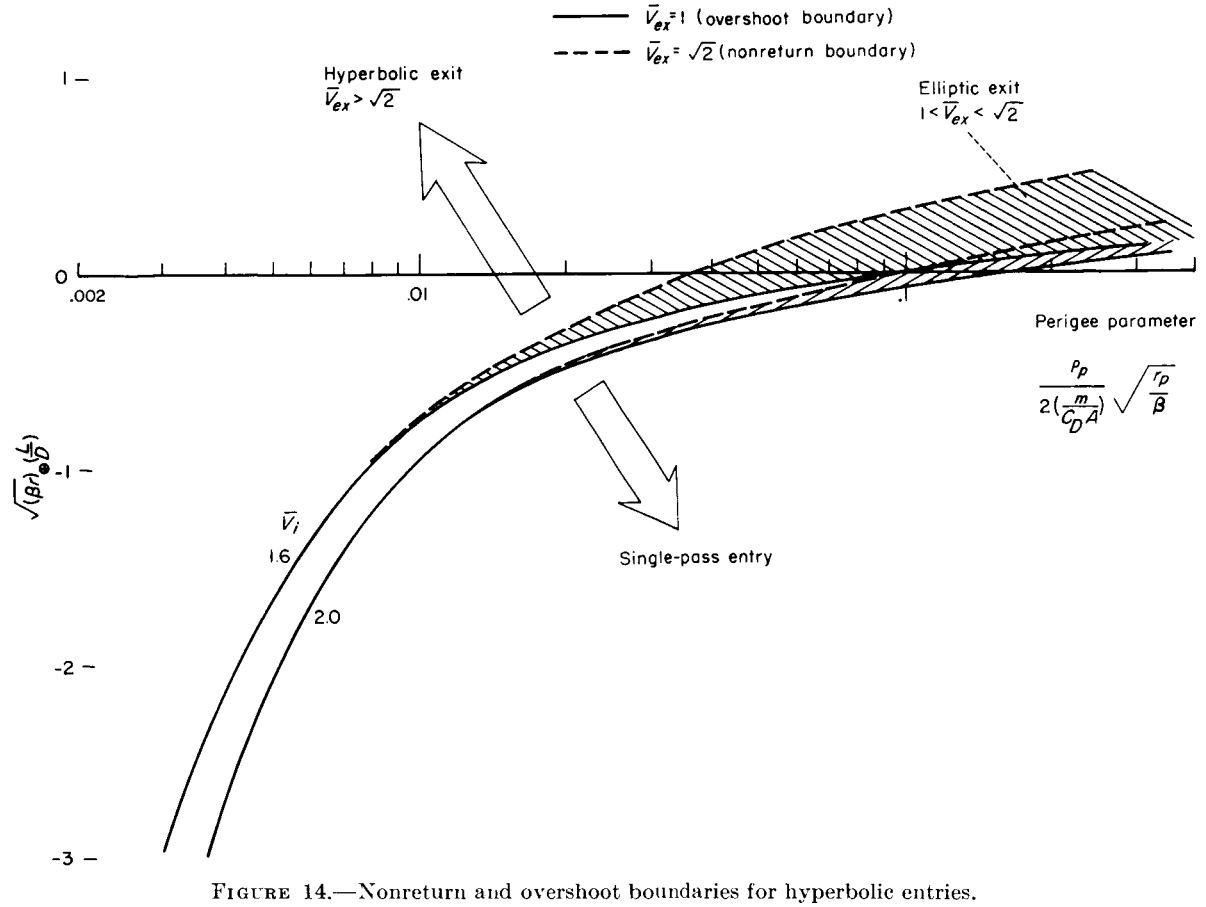

FIGURE 14.—Nonreturn and overshoot boundaries for hyperbolic entries.

for $\overline{V}_i=2.0$ being at $F_p=0.17$ and the nonreturn boundary at $F_p=0.10$. This difference would amount to 0.2 $\Delta_{10}y$, or to only 2 miles of altitude for the earth's atmosphere. It may perhaps be surprising that the overshoot boundary is so sharply delineated in the sense that an entry pass slightly beyond it would result in a sizable supercircular exit velocity, rather than in the completion of entry. This may be an important consideration in prescribing the design boundaries for the guidance and control system of a spacecraft.

The present calculations of the overshoot boundary for arbitrary m/C_DA and planetary atmospheres are in good agreement with some calculations made by Lees, Hartwig, and Cohen (ref. 1) for a vehicle having $m/C_DA=3.1$ slug ft^{-2} and entering the earth's atmosphere at 35,000 feet per second ($\overline{V}_i=1.36$). They presented their results in terms of the flight-path angle at an arbitrary altitude of 400,000 feet. According to the present method, the radius to conic perigee is determined by F_p, m/C_DA, and β from equation (10); the angle at $y=400{,}000$ feet is determined from equation (7) or (9). For their vehicle the following results are obtained:

L/D	Present method, γ at 400,000 ft, deg	Lees, et al., γ at 400,000 ft, deg
0	5.2	5.4
−1	4.4	4.4
−2	4.2	4.2

The agreement is quite satisfactory.

UNDERSHOOT BOUNDARY FOR LIFTING VEHICLES

A deceleration-limited undershoot boundary is affected not only by the maximum value of G selected, but also by the particular way in which the L/D is monitored. By "constant L/D" is meant an entry in which L/D is constant at least until the flight path is essentially horizontal ($\gamma\cong 0$, near where maximum horizontal deceleration is reached) and is reduced thereafter in order to complete entry in a single pass. By "modulated L/D," as introduced by Lees, Hartwig, and Cohen (ref. 1), is meant an entry in which L/D is monitored well before $\gamma=0$ is reached in the particular manner which maintains constant resultant deceleration.

The beneficial effects of modulated lift on deceleration and/or guidance requirements have been discussed by Lees, Hartwig, and Cohen under the assumption that m/C_DA is maintained constant as L/D is varied. They show that by modulating the L/D in a manner such that large L/D values are employed in the first portion of the entry where the longitudinal deceleration is small, the resultant deceleration can build up to its maximum under conditions where the transverse component ($\sim$ lift) is dominant. Then, by maintaining constant resultant G through decreasing the transverse component (decreasing $\sqrt{1+(L/D)^2}$) and increasing the longitudinal component, the entry with modulated lift can be completed without requiring large negative L/D's at any stage. In this way the undershoot boundary for modulated L/D can be extended considerably from the value for constant L/D, provided the value of L/D at entry is relatively high. Modulation, however, is not effective in extending the overshoot boundary. Overshoot is extended the most, as noted above, by setting a vehicle at $L/D\cong -0.5$ and then keeping this value constant until $\overline{V}_{ex}=1$ is reached.

In the present research, a large number of calculations have been made for the case of constant L/D. These calculations can be applied also to the case of modulated L/D by employing a result of Lees, Hartwig, and Cohen. They found that the ratio of G_{max} for modulated lift to G_{max} for constant lift was essentially independent of γ_i and V_i and dependent only on the value of L/D at entry. A curve showing their result is presented in figure 15. Since they found this curve to be independent of γ_i, it would be independent of the parameter $\sqrt{\beta r}\ \gamma_i$ and hence presumably can be applied to any planetary atmosphere. It should not be surprising that this curve varies almost as $[1+(L/D)^2]^{-1/2}$, inasmuch as the benefits of modulation in alleviating the resultant deceleration are obtained primarily by working with the transverse lift component. The curve in figure 15 is used in this report for obtaining undershoot boundaries for modulated L/D from curves calculated for constant L/D.

Curves are presented in figure 16 of the normalized maximum deceleration $\overline{G}_{max}$ as a function of $\log_{10}F_p$ for various $\overline{V}_i$ and constant L/D. The abscissa extends to much higher values of F_p (10^{40} for $\overline{V}_i=1.05$ and 1.1, corresponding to 400 miles altitude increment for the earth) than previously considered. The circle points represent the overshoot boundary for single-pass entries. From these working curves a deceleration-

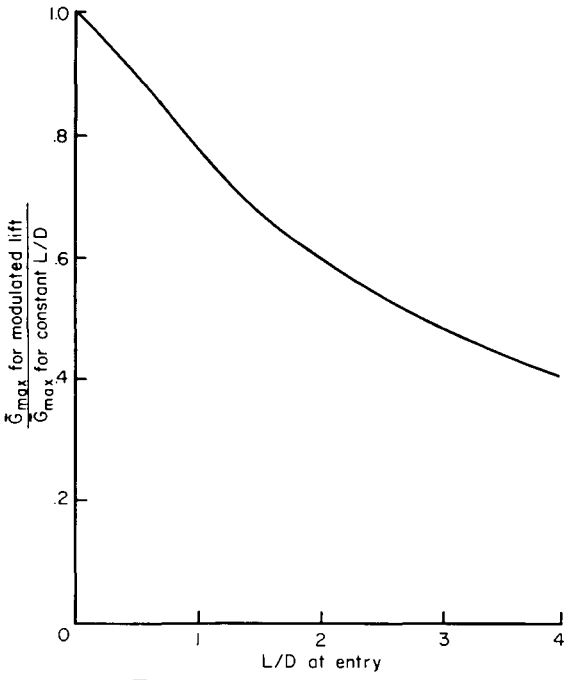

FIGURE 15.—Effect of modulated lift in reducing peak deceleration; from results of Lees, Hartwig, and Cohen (ref. 1).

limited undershoot boundary can be determined for a given G_{max}, L/D, and atmosphere. A heating-rate-limited undershoot boundary can be calculated approximately from the relationships developed in appendix A between G_{max} and convective heating.

It is apparent from figure 16 that an increase in L/D up to about 2 can extend considerably the undershoot boundary for a given $\overline{G}_{max}$. The magnitude of the extension in terms of log F_p would be proportional to the extension in altitude only if C_D were independent of L/D (the effect of C_D-L/D coupling is considered later). In the initial stages of entry into the atmosphere, the transverse lift force deflects the trajectory upward so that a lifting vehicle does not descend as rapidly into the lower layers of dense air as does a nonlifting vehicle. Hence, for a given F_p a lifting vehicle experiences less longitudinal deceleration than a nonlifting one. This beneficial effect of L/D increases only up to about $L/D=2$. Larger values of L/D (for the case of constant L/D entry) do not further extend the undershoot boundary because the adverse effect of the lift force in producing transverse deceleration dominates the beneficial effect of the deflected trajectory in reducing longitudinal deceleration. Over most of the range of L/D and F_p considered, a vehicle would exit from the atmosphere if the L/D were held constant during the entire entry. The vehicle can easily avoid exiting by reducing L/D after G_{max} has been experienced near the point where $\gamma=0$.

The curves in figure 16 for lifting vehicles represent the domain of shallow entries ($\gamma_i<10°$ in most cases for the earth) and of $L/D\leq 4$. Steeper entries, or those with $L/D>4$, correspond to conditions under which the gravity and centrifugal forces are small compared to the lift and vertical deceleration. Under such circumstances the approximate solution of Eggers, Allen, and Neice (ref. 5) for skip vehicles would apply. As shown in reference 2, this particular solution corresponds to a function Z_{III} given by

$$Z_{III}=\overline{u}\sqrt{\beta r}\left(\gamma_i \ln\frac{\overline{u}}{\overline{u}_i}-\frac{L}{2D}\ln^2\frac{\overline{u}}{\overline{u}_i}\right) \tag{30}$$

and to

$$G_{III_{max}}=\frac{g_\oplus(\sqrt{\beta r}\gamma_i)^2\overline{V}_i^2}{2(L/D)}\sqrt{1+\left(\frac{L}{D}\right)^2}\,e^{\frac{2\gamma_i}{L/D}} \tag{31}$$

$$q_{III_{max}}=\overline{V}_i^3\,(\beta r)^{1/4}\,e^{\frac{3\gamma_i}{L/D}}\,\frac{(-\gamma_i)}{\sqrt{2L/D}} \tag{32}$$

As in the case of steep nonlifting entries, the use of γ_i for steep lifting entries is probably more convenient than the use of F_p.

The present calculations of the undershoot boundary, like those of the overshoot boundary, can also be compared with calculations made by Lees, Hartwig, and Cohen for their specific conditions ($m/C_DA=3.1$ slug ft^{-2}, $\overline{V}_i=1.36$, earth's atmosphere, and γ defined as that at 400,000 ft). For this comparison the 10 G_{max} boundary is selected, with the following results:

L/D	Present method γ at 400,000 ft, deg	Lees, et al., γ at 400,000 ft, deg
0	5.8	5.8
.5	7.4	7.7
2	8.2	8.5
2 modulated	9.8	10.6

The agreement is regarded as satisfactory.

CORRIDOR WIDTH FOR LIFTING VEHICLES

Single-pass entries.—In figure 17 curves are shown of both the overshoot and undershoot boundaries for shallow entries into the earth as a function of $|L/D|$ for $\overline{G}_{max}$ of 5, 10, and 20, and for various $\overline{V}_i$. These two boundaries determine the single-pass corridor width. For a given value of

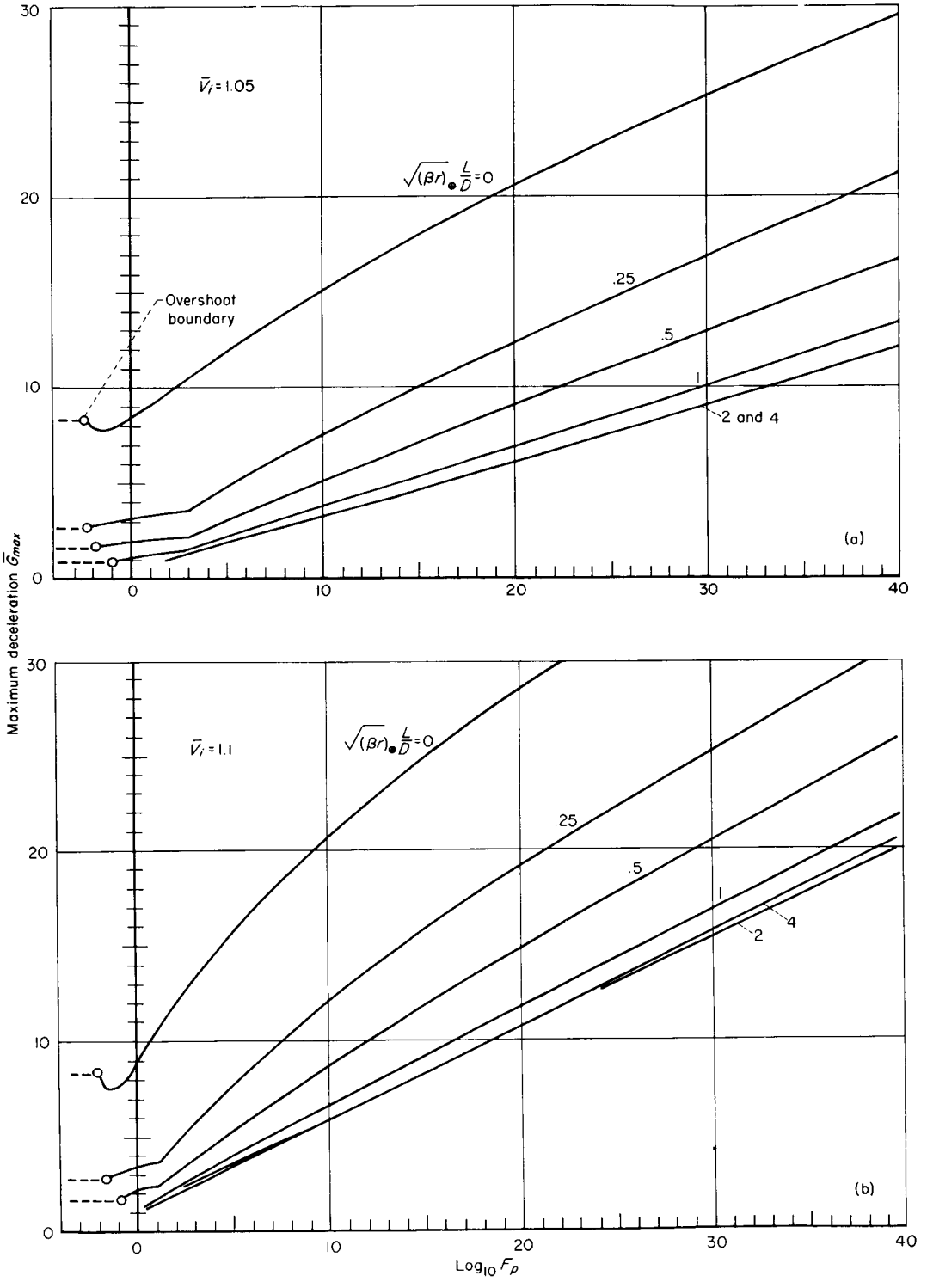

(a) $\overline{V}_i = 1.05$
(b) $\overline{V}_i = 1.1$

FIGURE 16.—Normalized maximum deceleration for various lift-drag ratios and entry velocities.

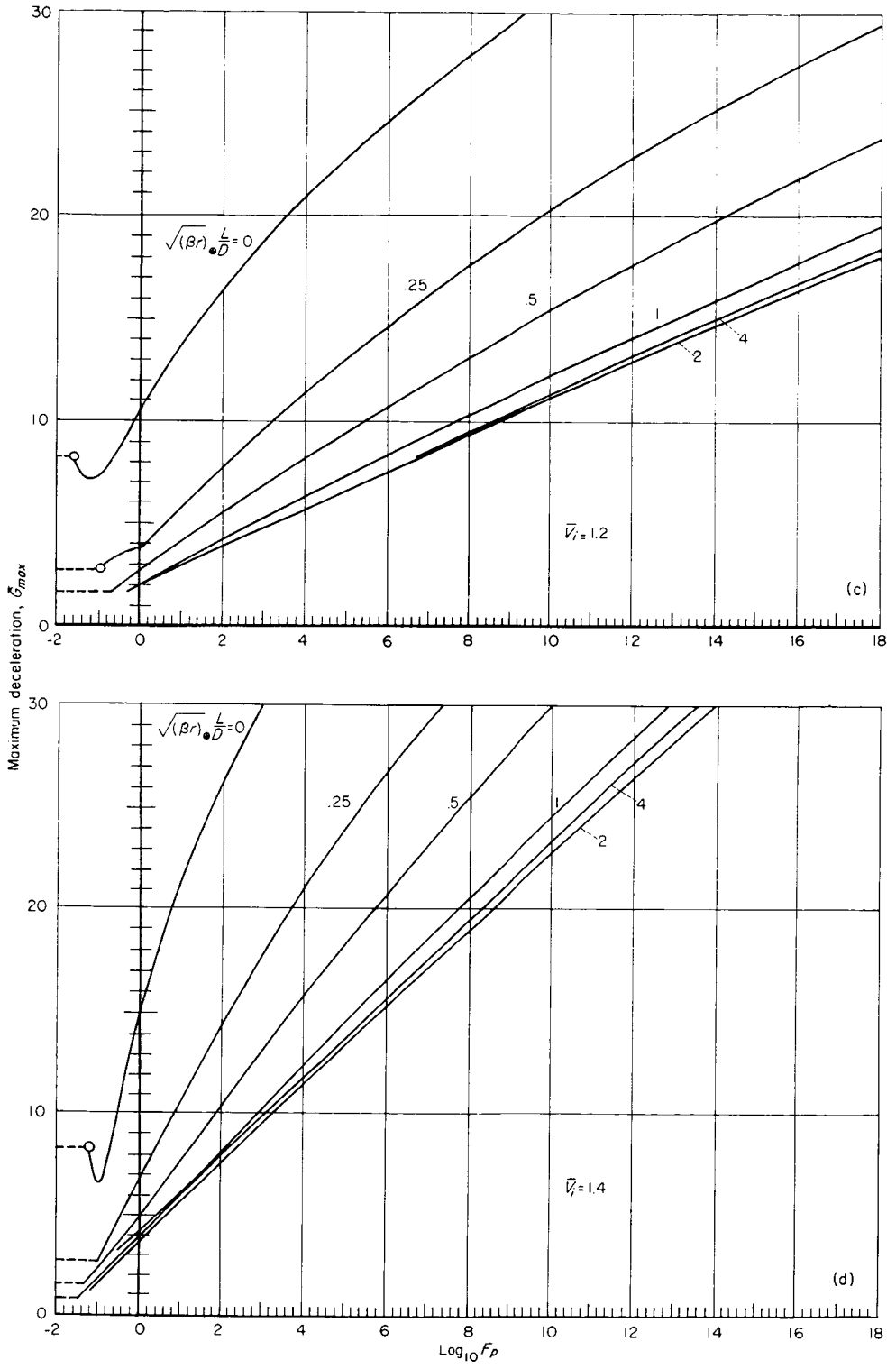

(c) $\overline{V}_i=1.2$
(d) $\overline{V}_i=1.4$

FIGURE 16.—Continued

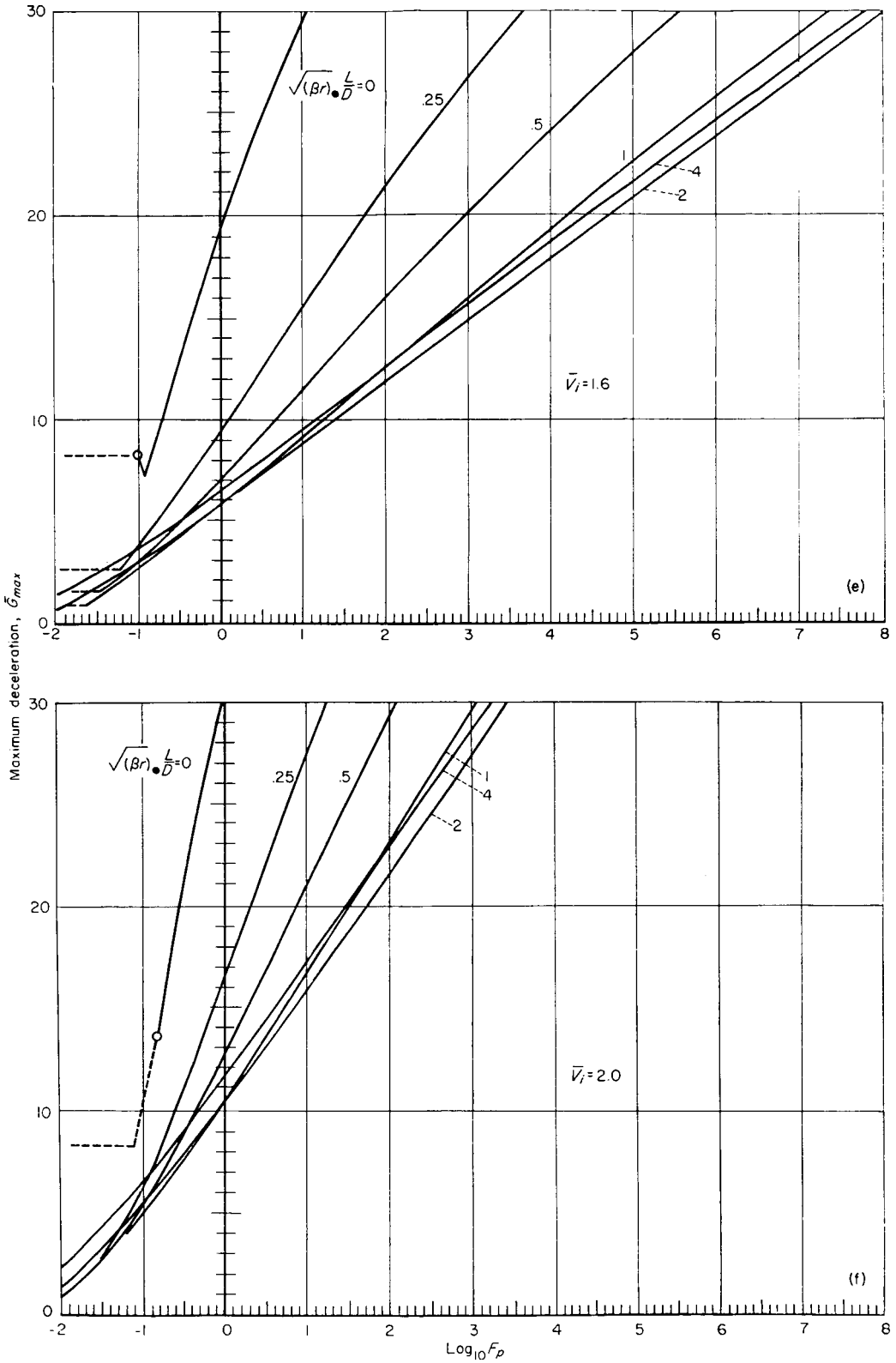

(e) $\bar{V}_i=1.6$
(f) $\bar{V}_i=2.0$

FIGURE 16.—Concluded.

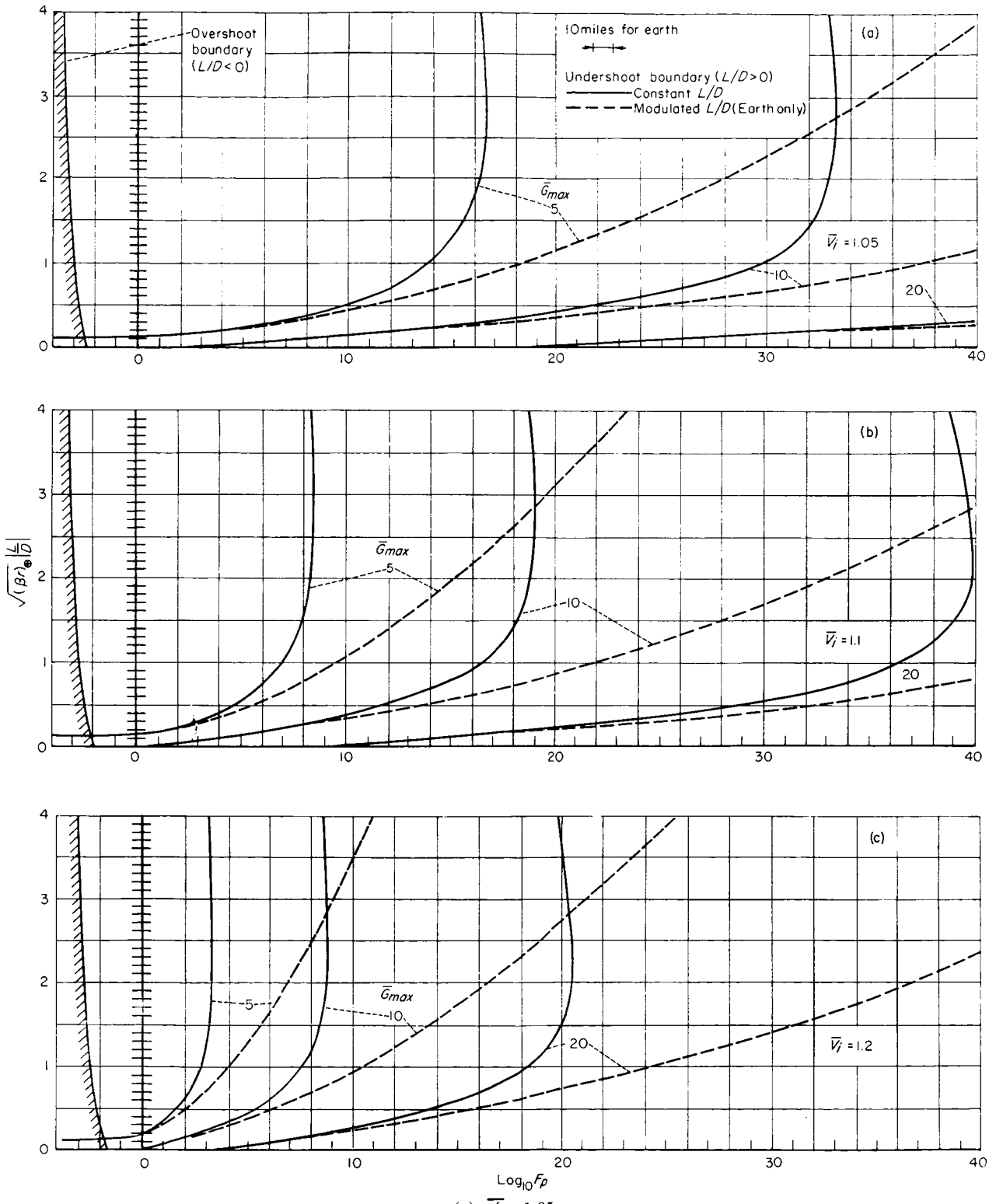

(a) $\bar{V}_i = 1.05$
(b) $\bar{V}_i = 1.1$
(c) $\bar{V}_i = 1.2$

FIGURE 17.—Overshoot and undershoot boundaries as a function of lift-drag ratio for various entry velocities and maximum deceleration.

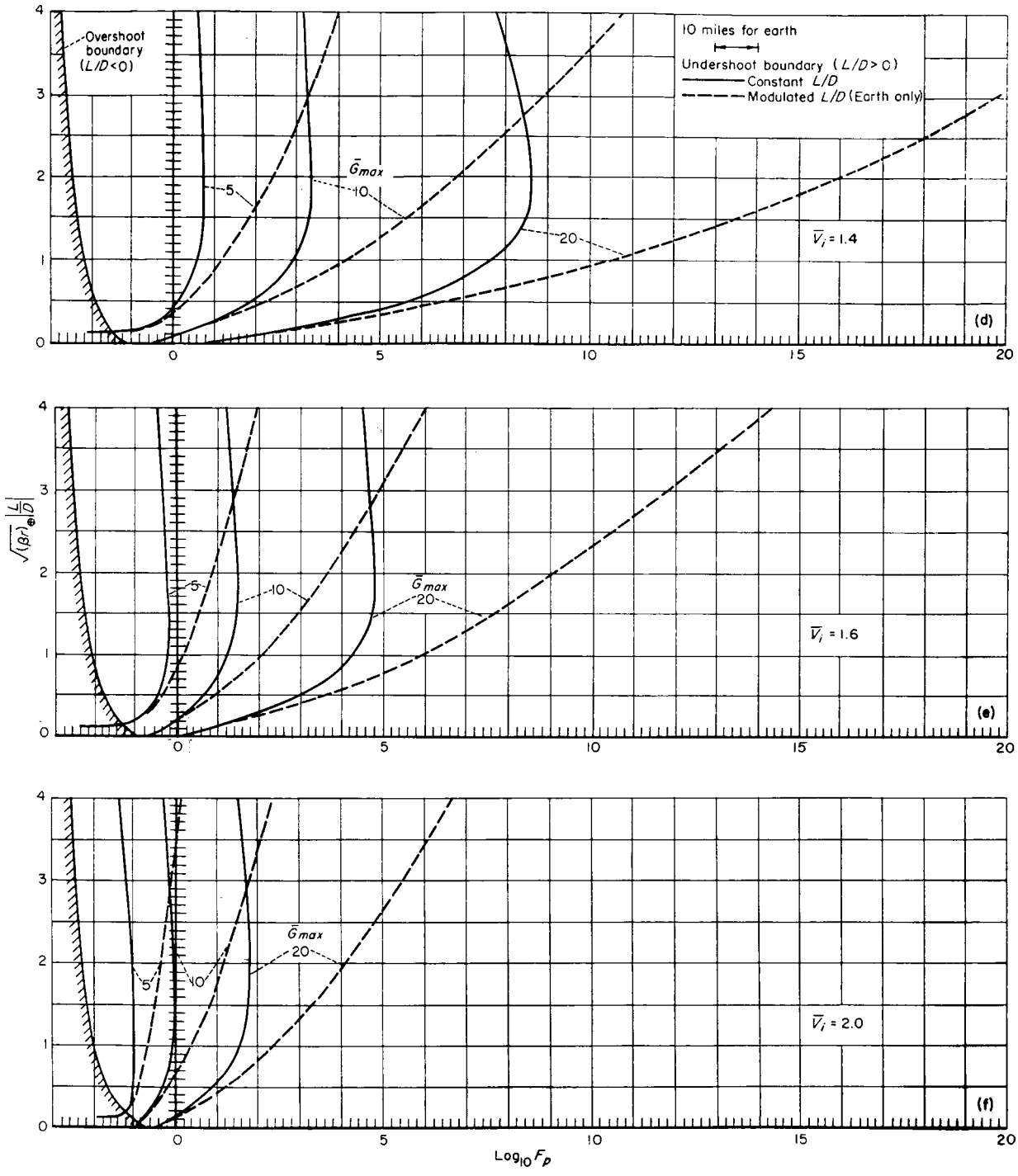

(d) $\bar{V}_i = 1.4$

(e) $\bar{V}_i = 1.6$

(f) $\bar{V}_i = 2.0$

FIGURE 17.—Concluded.

|L/D|, the overshoot boundary would represent $L/D<0$, and the undershoot $L/D>0$. The solid curves identified as constant L/D, as noted previously, correspond to L/D fixed during entry only until $\gamma\cong 0$, and to L/D monitored in some unspecified way thereafter in order to complete entry in a single pass; the dashed curves identified as modulated L/D, represent a fixed L/D only for a much shorter portion of the entry, and to L/D monitored well before the $\gamma=0$ point is reached. With a given $\overline{G}_{max}$ the undershoot boundaries are seen to be about the same for constant L/D as for modulated L/D in the range of $|L/D|$ less than about 0.5. At L/D greater than about 1, the undershoot boundaries with modulated L/D are considerably extended beyond those for constant L/D.

For vehicles having a fixed C_D independent of L/D, the effect of L/D on corridor width can be visualized from the spacing between overshoot and undershoot boundaries, inasmuch as $\Delta y_p = \Delta_{10}y(\log_{10}F_{p_{un}} - \log_{10}F_{p_{ov}})$ for such vehicles. Inspection of the spacing between the log F_p boundaries in figure 17 shows that the corridor width for the case of constant L/D attains a maximum at L/D between about 2 and 3, but for the case of modulated L/D increases indefinitely as L/D increases. The corridor width for modulated L/D at $(L/D)_{\text{entry}}=3$ (and C_D independent of L/D), for example, is essentially double that for constant L/D over the entire range considered in figure 17 ($5\leq G_{max}\leq 20$ and $1.05\leq \overline{V}_i\leq 2.0$). Some example values corresponding to C_D independent of L/D are as follows:

	Corridor width in miles for $\overline{V}_i=1.4$								
	5 G_{max}			10 G_{max}			20 G_{max}		
	$\frac{L}{D}=0$	$\frac{L}{D}=1$	$\frac{L}{D}=1$ modulated	$\frac{L}{D}=0$	$\frac{L}{D}=1$	$\frac{L}{D}=1$ modulated	$\frac{L}{D}=0$	$\frac{L}{D}=1$	$\frac{L}{D}=1$ modulated
Venus	0	27	36	8	52	70	26	105	140
Earth	0	27	34	7	51	65	20	100	130
Mars	210	300	370	400	550	720	1250	1240	1740
Jupiter	0	34	42	0	52	70	0	90	120

Corridor widths for Titan are not listed since they correspond to such steep entries that aerodynamic lift is ineffective in broadening the corridor width beyond the values already tabulated for $L/D=0$. Even in the case of Mars, the parabolic entry angle for 20 G_{max} is sufficiently steep (47°) that the reduction in longitudinal force brought about by the deflected trajectory is overweighed by the transverse lift force producing the deflection, so that the net effect is a greater resultant deceleration (and narrower corridor) for $L/D=1$ than for $L/D=0$. Modulated L/D, though, still appears to provide a moderate broadening of the Mars corridor, but this is based on the untested assumption that the curve of figure 15 applies to steep as well as shallow entries. The figures for Mars in the above table include a 100-mile increment for the conic perigee altitude of overshoot. This particular increment corresponds to $(m/C_DA)_{ov}=1$ slug/sq ft, $(L/D)_{ov}=-0.5$, and to a surface-level atmosphere density on Mars of 0.0002 slug/cu ft.

Because of guidance errors, a spacecraft may unavoidably enter either near overshoot or undershoot. A lifting vehicle could employ a different $\overline{L/D}$ if entry occurred near overshoot than if it occurred near undershoot, and could have greatly different C_D at these two boundaries. It is of interest, then, to consider the interdependence of C_D and L/D in order to evaluate the practical effectiveness of L/D in broadening the entry corridor. We will assume that $L/D=-0.5$ at overshoot, since this value produces the highest overshoot boundary when the C_D-L/D coupling is considered. At undershoot we will assume that any constant L/D equal to or less than 4 could be employed. From equation (18) for the corridor width it follows that with m/A fixed,

$$\Delta y_p = \Delta_{10}y\left[\log_{10}\left(\frac{F_p}{C_D}\right)_{un} - \log_{10}\left(\frac{F_{p_{ov}}}{C_D}\right)_{L/D=-0.5}\right] \tag{33}$$

The values of F_p can be obtained from figure 17,

and C_D from values of $C_D/C_{D_{max}}$ tabulated in appendix B (taking $C_{D_{max}}=1.7$, for example). In making comparison with the case of C_D independent of L/D, we will consider two entries: (1) entry with L/D at undershoot different from that at overshoot, but with C_D independent of L/D, and (2) the same entry, only with C_D dependent on L/D. For convenience, the invariant C_D of case (1) will be taken as equal to the $C_{D_{un}}$ of case (2). In the case (2) with C_D-L/D coupling, the overshoot boundary would be higher than in case (1) because $L/D=-0.5$ produces the highest overshoot altitude when the C_D-L/D coupling is considered. In the range of $(L/D)_{un}$ between about 0.25 and 1, C_D is not greatly different than at $L/D=-0.5$; for practical purposes, then, the corridor widths in this range of $(L/D)_{un}$ are essentially the same as those previously computed under the assumption that C_D is independent of L/D. Because of two compensating effects, the corridors tabulated above for $L/D=1$ and C_D independent of L/D are also closely representative of those for C_D-L/D coupling with $(L/D)_{un}=1$ and $(L/D)_{ov}=-0.5$. Compensating effects occur because at $(L/D)_{ov}=-0.5$, C_D is double that at $(L/D)_{un}=1$, but log $F_{p_{ov}}$ also is double. The corridors for higher $(L/D)_{un}$, however, can be considerably broader than if calculated under the assumption of C_D independent of L/D. Calculations from equation (33) of the 10 G_{max} corridor width for parabolic entry into various planets, including the influence of C_D-L/D coupling, and the assumption that $L/D=-0.5$ at overshoot, yield the following values:

$(L/D)_{un}$	Corridor width in miles, $\overline{V}_i=1.4$							
	Venus		Earth		Mars		Jupiter	
	Constant L/D	Modulated L/D	Constant L/D	Modulated L/D	Constant L/D	Modulated L/D	Constant L/D	Modulated L/D
1	53	67	52	66	550	720	55	70
2	63	99	62	97	520	920	77	110
4	71	149	71	146	480	1300	93	160

The relatively broad corridors for $(L/D)_{un}=4$, unfortunately, are associated with severe heating penalties, particularly in the case of modulated L/D. This association is discussed later.

A pronounced trend of decreasing corridor width with increasing entry velocity can be seen from comparison of the various portions of figure 17, but it is more apparent from the cross plot in figure 18 where $\overline{V}_i$ is employed as the ordinate. Each plot is for various values of $\overline{G}_{max}$ and for a different value of $\sqrt{(\beta r)_\oplus}(L/D)$, and can be applied to any planet for $\overline{V}_i \geq 1.05$ approximately. For V_i too near 1.0, the planetary similarity in terms of F_p as the correlating parameter breaks down, and the curves in the region $1.05>\overline{V}_i\geq 1.0$ are, strictly speaking, those for Earth only (or Venus with $\sqrt{(\beta r)_\oplus}\cong 1$) as previously pointed out. The dashed curves representing modulated lift depend on the individual values of both L/D and $\sqrt{(\beta r)_\oplus}(L/D)$ for all $\overline{V}_i$, and apply only to $\sqrt{\beta r}=30$ (Earth, Venus). It is evident, for example, that the Earth 10 G_{max} corridor width for non-lifting vehicles decreases from about 180 miles at $\overline{V}_i=1$ (circular entry) to 7 miles at $\overline{V}_i=\sqrt{2}$ (parabolic entry), to 0 miles at $\overline{V}_i\geq 1.8$. For constant $L/D=1$, the corresponding widths are about 560 miles at $\overline{V}_i=1$, 50 at $\overline{V}_i=\sqrt{2}$, and 20 at $\overline{V}_i=2.0$. Clearly, any increase in entry velocity not only increases the amount of heat to be absorbed, but also increases the severity of the guidance requirements to be met by a manned spacecraft which is deceleration-limited.

Multiple-pass entries.—Thus far consideration has been given only to the corridor for single-pass entry. Multiple-pass atmosphere-braking entries are of interest for several reasons, one of which is that they provide a means of minimizing aerodynamic heating. For example, in an entry which first makes a number of supercircular passes through the outer edge of atmosphere until the velocity is reduced to circular velocity, and then completes the subcircular portion of entry with a sizable positive L/D, the decelerations experienced—and, hence, also the rates of aerodynamic

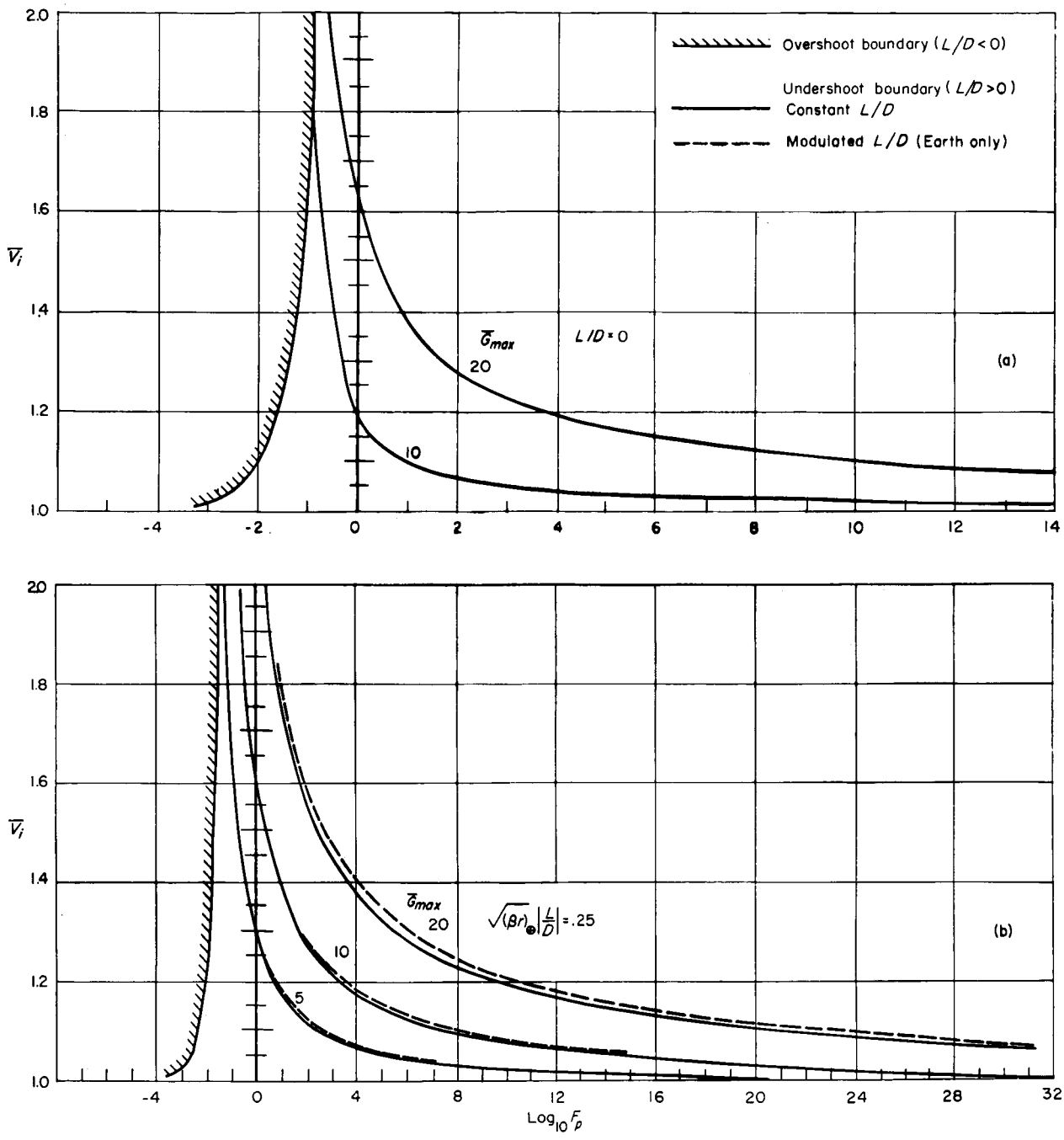

(a) $\sqrt{(\beta r)_\oplus}\, L/D=0$

(b) $\sqrt{(\beta r)_\oplus}\, L/D=0.25$

FIGURE 18.—Overshoot and undershoot boundaries as a function of entry velocity for various lift-drag ratios and maximum deceleration.

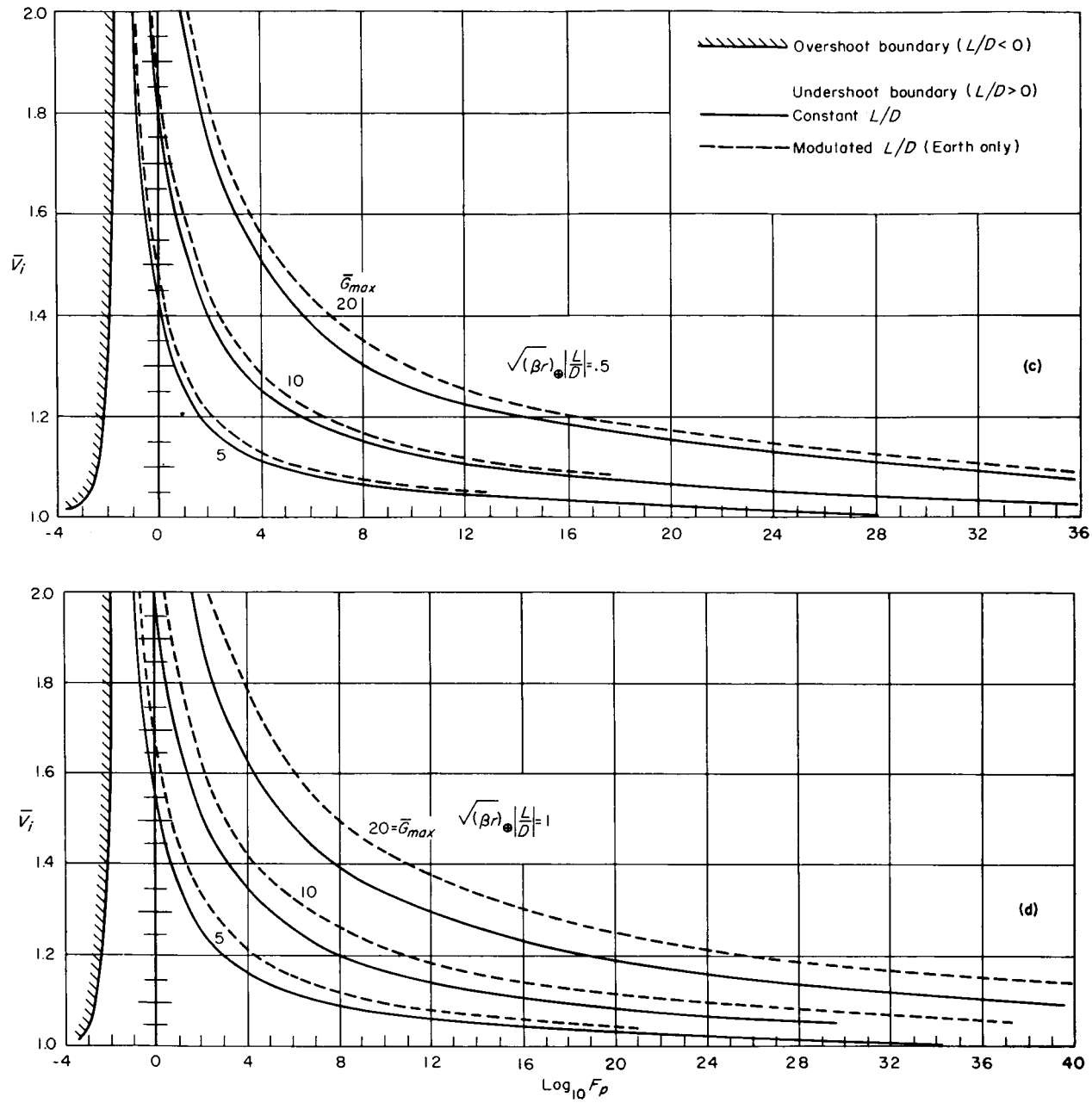

(c) $\sqrt{(\beta r)_\oplus}\, L/D=0.5$

(d) $\sqrt{(\beta r)_\oplus}\, L/D=1$

FIGURE 18.—Continued.

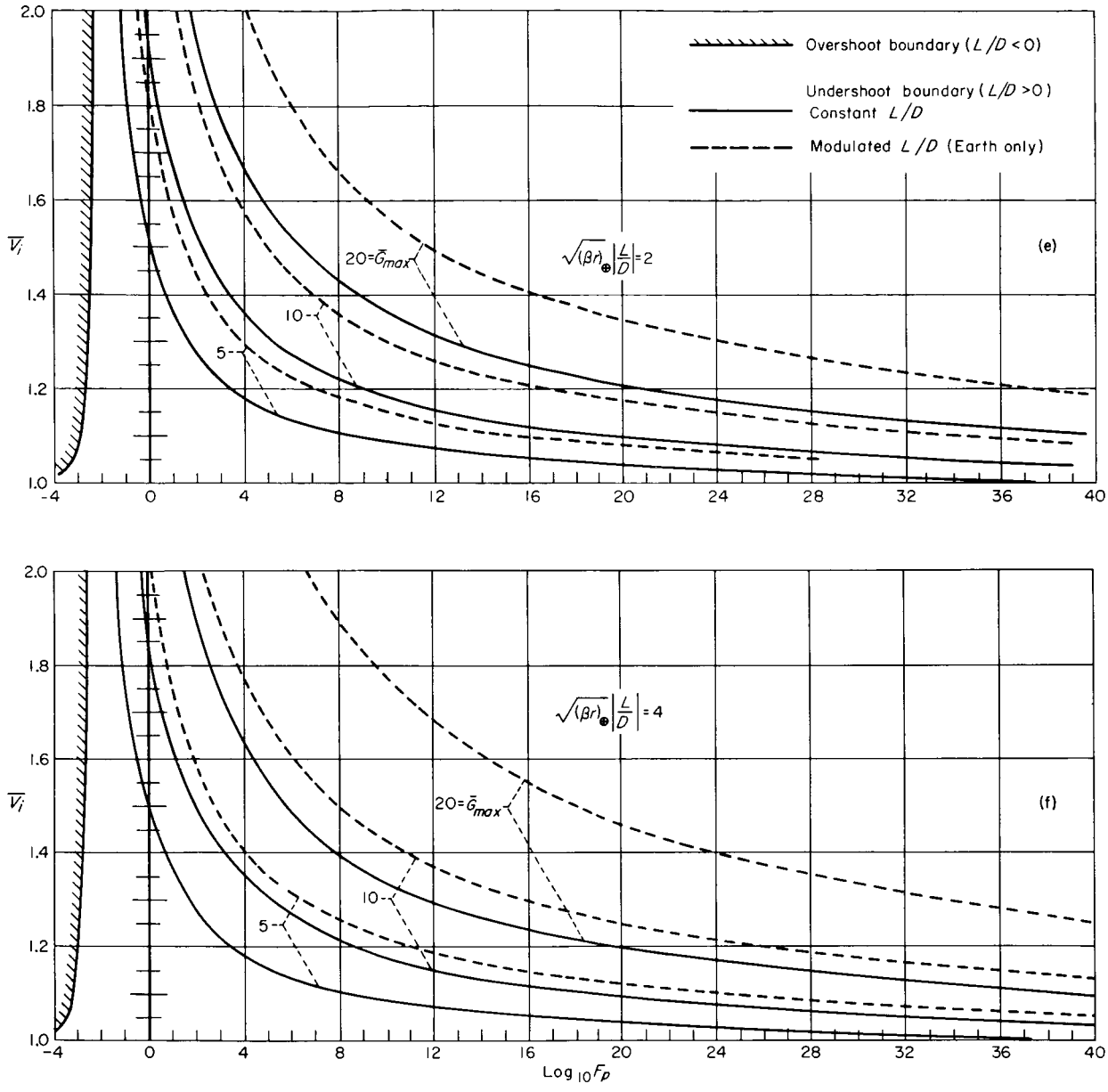

(e) $\sqrt{(\beta r)_\oplus}\, L/D=2$

(f) $\sqrt{(\beta r)_\oplus}\, L/D=4$

FIGURE 18.—Concluded.

heating—can be kept relatively small throughout the entry. It was shown in reference 2 that with $L/D=0$ six supercircular passes would be required to keep the maximum heating rates about the same as that experienced during the terminal subcircular portion of the entry. Since each pass is followed by a substantial period wherein the structure may cool as the vehicle orbits in preparation for a subsequent pass, this provides an attractive possibility for utilizing the combined heat-sink-radiation capacity of a structure.

At least two important problems would arise if multiple-pass atmosphere brakings were attempted. First, they would require multiple passes through the radiation belt around any planet, and second, they can require a relatively

accurate entry guidance system. The guidance accuracy required may be deduced from the following results for parabolic entry (approximate F_p boundaries have been determined by interpolation from a number of solutions of the entry-motion differential eq. (3)):

Number of passes to complete entry	F_p boundaries		
	$L/D=-1$	$L/D=0$	$L/D=1$
1	∞	∞	∞
2	0. 006	0. 06	10^{10}
3	. 005	. 03	10^{2}
4	. 0046	. 02	1
	. 004	. 013	0. 2

It follows, for example, that the corridor width for completion of parabolic entry without lift on the third pass would be $\Delta_{10}y\ \log_{10}(0.03)/(0.02)=0.18\ \Delta_{10}y$, which represents a 1.8 mile wide corridor in the earth's atmosphere. For $L/D=-1$ the corresponding 3-pass Earth corridor width would be 0.4 mile, and for $L/D=1$, 20 miles. The corridor widths for 6-pass entries would be considerably smaller. If one did not specify the number of passes, but only that the maximum heating rate in the first pass not significantly exceed the value for sub-circular orbital decay, the resulting corridor widths also would be correspondingly narrow. Thus, with $L/D=0$, $\overline{q}_{max}$ is 0.22 in orbital decay (see fig. 7), and for $0.22 \leq \overline{q}_{max} \leq 0.24$ the guidance requirement of a parabolic approach would be $0.0056 \leq F_p \leq 0.0080$; this corresponds to an Earth corridor width of about 1.6 miles. When the narrow corridors are considered together with the possible shielding weight penalty for protecting an occupant during repeated passes through the radiation belt, it would appear that multiple-pass atmosphere-braking entries which require a large number of passes are of restricted attraction, at least for parabolic entry into Earth. Two-pass atmosphere braking, however, corresponds to a rather broad corridor (8 $\Delta_{10}y$, as may be deduced from the above table) and may be of considerable interest.

A second reason why multiple passes are of interest is that they offer a possible means of achieving flexibility in selecting the time and the area upon which a spacecraft lands. After a hyperbolic or parabolic approach has been converted to a slightly elliptic orbit of relatively short period, a spacecraft could orbit until the earth's rotation turns a desirable landing area into the proper position relative to the plane of the orbit for making a landing. The apogee altitude of the slightly elliptical orbit around the earth would have to be less than about 1000 miles, however, if the inner radiation belt were to be avoided; this restricts the exit velocity from the first supercircular pass to $\overline{V}_{ex}<1.05$ approximately. At the same time the exit velocity would have to be supercircular in order to have at least one orbit before landing. The resulting corridor, limited by $1.0<\overline{V}_{ex}<1.05$ is narrow, but not impossibly narrow if a lifting vehicle possesses the capability of programing L/D during entry in a number of different ways (depending on the particular conic perigee of the approach trajectory) and if it also possesses the trajectory-intelligence capability of knowing upon what trajectory it is approaching after the terminal-guidance correction is made so as to thus be able to select a proper mode of L/D modulation. That this is so may be deduced from figure 19 showing dotted lines of constant $\overline{V}_{ex}$ and solid lines of constant G_{max}. All curves apply to a fixed L/D during entry. The parabolic corridor undershoot boundary producing $1.0<\overline{V}_{ex}<1.05$, and also $\overline{G}_{max}=10$, is at $\log_{10}F_p=2.1$, and at $L/D\cong 0.6$. The corridor overshoot boundary limited only by $\overline{V}_{ex}<1.05$ is at $\log_{10}F_p=-1.9$ if $L/D=-0.5$ at overshoot. The resulting earth corridor width is 40 miles. If a spacecraft enters near undershoot with $L/D=2$ and rapidly reduces L/D immediately after G_{max} is experienced in a special program such that enough deceleration is encountered to produce $\overline{V}_{ex}<1.05$, then the undershoot boundary could be extended to $\log_{10}F_p=3.2$, which occurs at about 11 miles lower altitude than for $L/D=0.6$. The marked sensitivity of $\overline{V}_{ex}$ to small changes in F_p at negative L/D, as noted earlier, is also evident in figure 19.

At least two operational complications would arise if a vehicle attempted to utilize these 40 or 51 mile corridor widths for the conversion from parabolic approach to a tight elliptical orbit. First, a small rocket thrust would have to be

exerted when first reaching apogee after the initial grazing pass in order that the spacecraft have a reasonable lifetime as an orbiting satellite (otherwise any entry near undershoot would be completed on the second pass). Second, each value of F_p within the boundaries would require a different mode of L/D programing in order to always exit in the desired range $1.0<\overline{V}_{ex}<1.05$. If an appropriate L/D programing were not employed for the particular F_p of an approach trajectory, the corridor would be much narrower. From figure 19(a) we see, for example, that if a fixed L/D were maintained, it could be no greater than 0.45 for $\overline{G}_{max}=10$, and the corresponding boundary would be $1.0<\log_{10}F_p<1.7$, representing an Earth corridor only 7 miles wide. To utilize

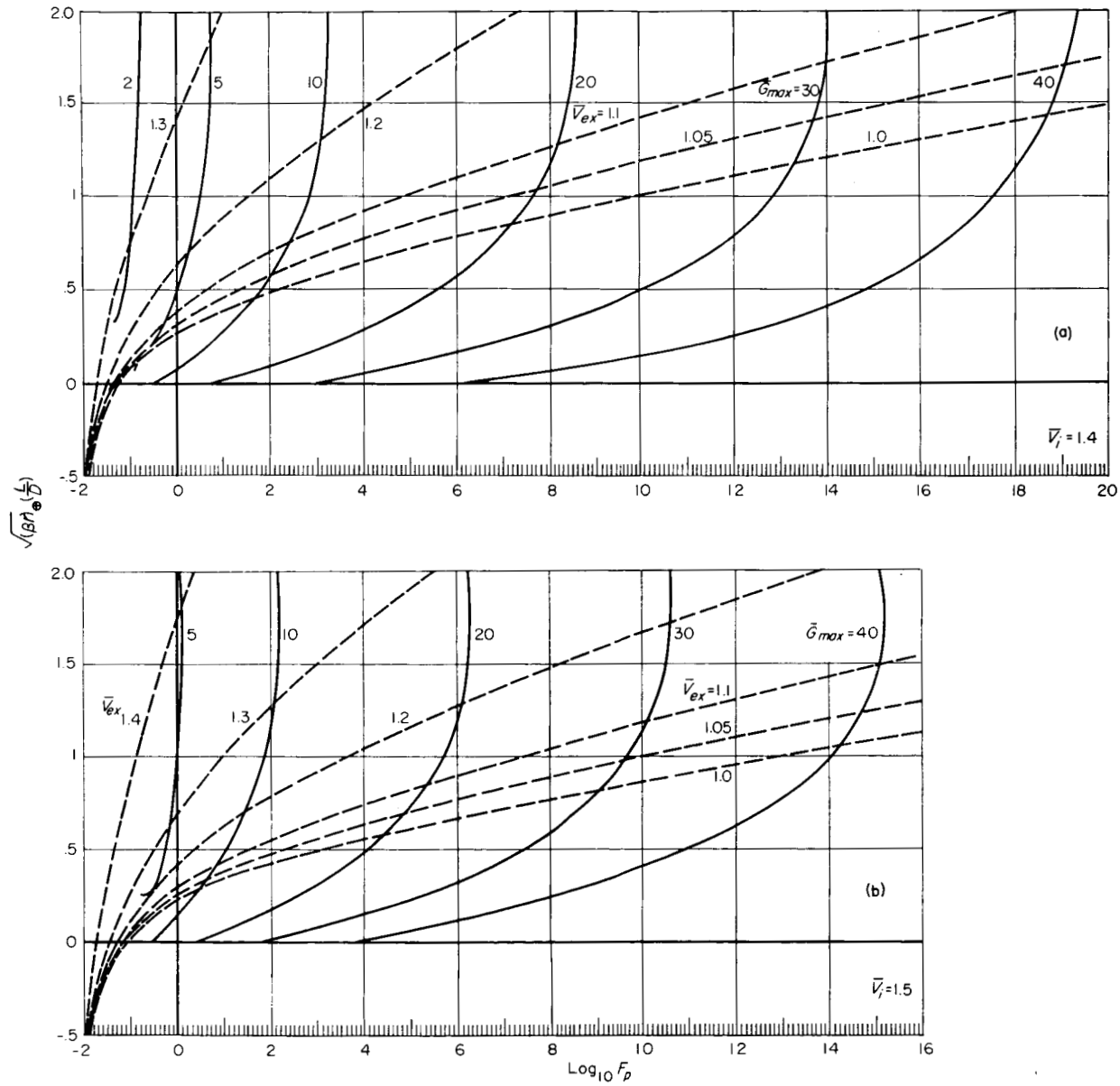

(a) $\overline{V}_i=1.4$

(b) $\overline{V}_i=1.5$

FIGURE 19.—Dimensionless exit velocity and maximum deceleration for atmosphere braking passes at hyperbolic and parabolic entry velocities.

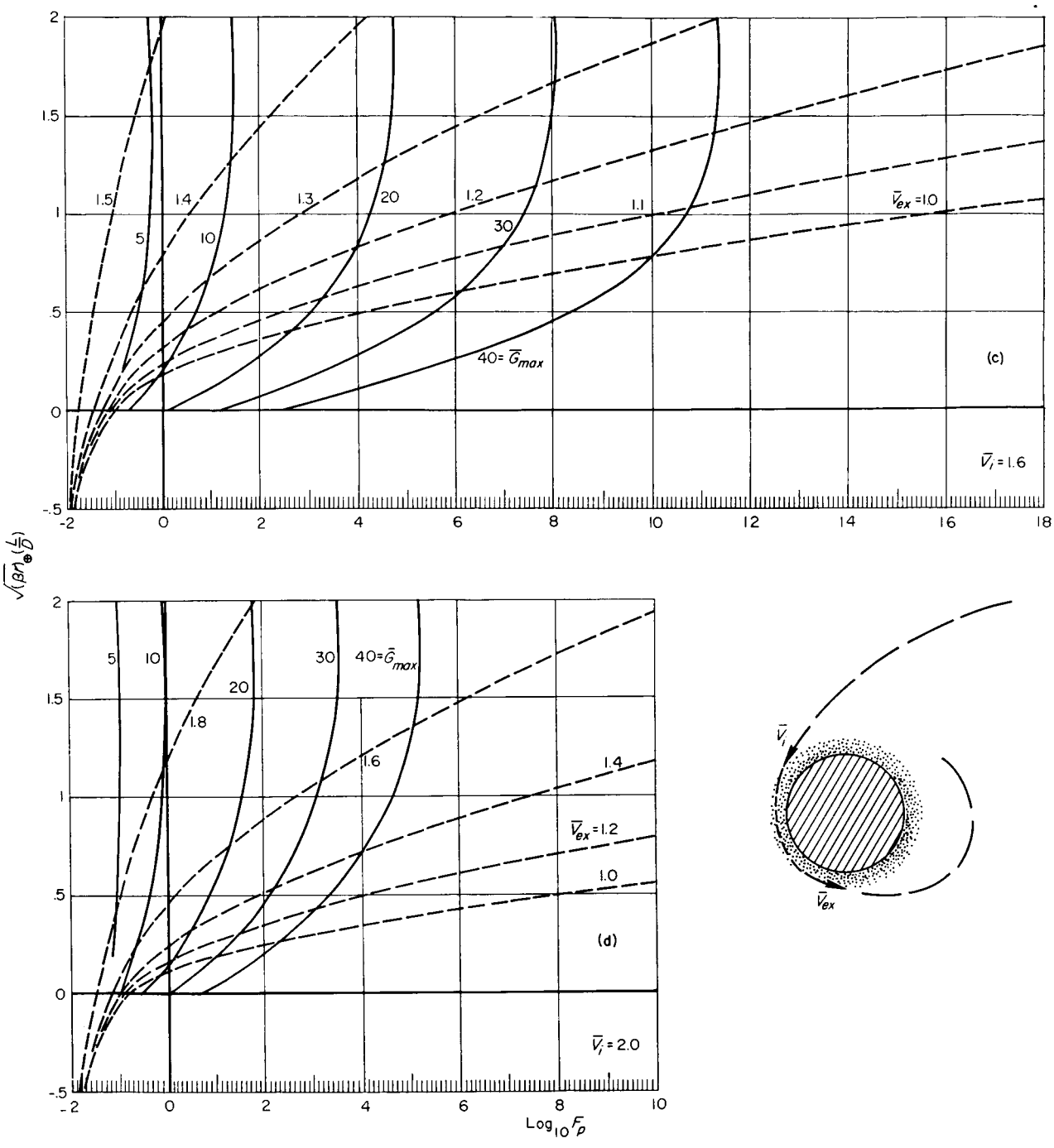

(c) $\bar{V}_i = 1.6$

(d) $\bar{V}_i = 2.0$

FIGURE 19.—Concluded.

the 40 or 51 mile corridor, then, would require that the spacecraft know what trajectory it is approaching on after the last terminal-guidance rocket is fired, and that it have the capability of variable L/D programing to suit; the L/D program appropriate for $\log_{10}F_p$ near 2 (near undershoot) would be very different from that for $\log_{10}F_p=-2$ (near overshoot.)

A different—and perhaps the most important—reason for interest in multiple supercircular passes is that they provide a possible method of reducing markedly the required Earth lift-off weight for interplanetary flights employing chemical propulsion. On a minimum-energy trip to Mars, for example, the heliocentric velocity of Mars would exceed that of the spaceship (when the spaceship arrived at Mars) by about 9000 feet per second. Without having to expend any fuel (but perhaps having to ablate a very small mass), this velocity increment could be achieved—disregarding guidance problems for the moment—by letting an edge of the Mars atmosphere "run into" the spacecraft in a certain manner. Relative to Mars, the spacecraft would enter the atmosphere at a hyperbolic velocity of about $\overline{V}_i=1.6$, and, if the spacecraft were guided toward the proper conic perigee so as to exit from the atmosphere somewhere in the elliptic range $1.0<\overline{V}_{ex}<1.3$, it would become a reasonable satellite of Mars. A small rocket impulse upon first reaching the ellipse apogee could then either induce entry if fired as a retrorocket, or greatly lengthen the lifetime of the spaceship as a Mars satellite if fired as a thrust rocket. Conversely, after a spacecraft returns to Earth from Mars the excess heliocentric velocity as it overtakes the earth (in this case, about 10,000 feet per second for a minimum energy trajectory) could be eliminated by guiding the spaceship toward the proper conic perigee so as either to land or to convert its hyperbolic entry velocity relative to earth ($\overline{V}_i=1.46$) to elliptic. By recalling that the Earth lift-off weight for chemical propulsion varies essentially exponentially with the over-all velocity increment which must be produced, it is not necessary to make numerical calculations to realize that an over-all round-trip saving of 19,000 feet per second in velocity increment would amount to a marked reduction in Earth lift-off weight. This reduction is achieved with only minor increases in the aerodynamic heating since $\overline{V}_i=1.46$ is only slightly greater than for parabolic entry. Similar comments apply, of course, to Earth-Venus and other journeys.

For small celestial objects like Mars, the entry guidance requirements to effect this desired hyperbolic-elliptic orbital transfer are much less severe than for Earth or Venus. Some numbers illustrating this can be obtained from figure 19. By employing $|L/D|\leq 2$ in Mars (no more severe heating than for $L/D=1$ in Earth) a G_{max} of 10 would correspond to $\overline{G}_{max}=44$ for Mars (eq.(25) with $\sqrt{(\beta r)_\oplus}=0.47$, $g_\oplus=0.38$). With $\sqrt{\beta r_\oplus}(L/D)=0.94$ the inner corridor boundary for $\overline{V}_i=1.6$ would be deceleration-limited at $\log_{10}F_p=12$, producing $\overline{V}_{ex}=1.03$. A reasonable outer boundary with this fixed $L/D=2$ would be at $\log_{10}F_p=2.5$ producing $\overline{V}_{ex}\cong 1.3$. Hence $\Delta y_p=\Delta_{10}y(9.5)=250$ miles in the Mars atmosphere. If the spaceship has the capability of programing L/D in a fashion tailored to the particular F_p it happens to be entering on, this corridor could be broadened about 100 miles more. Relative to the radius of Mars, such corridors are much broader than the parabolic-entry corridor into Earth from a return Moon journey (50 to 60 miles wide). Thus hyperbolic-elliptic orbital transfer by the atmosphere of Mars appears quite practical. Upon returning to Earth, though, the 10 G_{max} corridor width with fixed $L/D\cong 0.4$ for the analogous hyperbolic-elliptic transfer would be only about 29 miles (at $\overline{V}_i=1.46$ as interpolated between curves for $\overline{V}_i=1.4$ in fig. 19(a) and for $\overline{V}_i=1.5$ in fig. 19(b)), thereby imposing a guidance requirement about one order of magnitude more severe than in the case of Mars. The corresponding corridor width with variable L/D programing would be about 46 miles. Such corridors, however, may not impose impractically severe guidance requirements.

If a vehicle returns from a voyage to a distant point in the solar system, the relative hyperbolic velocity of entry into the earth's atmosphere would correspond to about $V_i\cong 2$. As may be deduced from figure 19(d), and as would be anticipated from results previously presented, the guidance requirements in this case for using the atmosphere to convert the spaceship to an orbiting earth satellite in the range $1.0<\overline{V}_{ex}<1.3$

would be quite severe. Even by assuming that the appropriate L/D programing could be achieved for any F_p, the 10 G_{max} corridor width would be only about 18 miles. The saving in Earth lift-off weight would indeed be sizable, though, since the excess heliocentric velocity, which need not be compensated for by expending rocket fuel, is about 40,000 feet per second in this case.

AERODYNAMIC HEATING AT CORRIDOR BOUNDARIES AND HEATING PENALTY ASSOCIATED WITH LIFTING VEHICLES

Aerodynamic heating at overshoot boundary.— Inasmuch as deceleration is at its minimum for single-pass entries along the overshoot boundary, the heating rate is also at its minimum (but the total heat absorbed is at its maximum). Considering that the maximum wall temperature varies as $q_{max}^{1/4}$ for a radiation-cooled vehicle, the approximate relationship (A13) between heating rate and deceleration should suffice for many engineering purposes in calculating wall temperatures of such vehicles. Curves of the dimensionless quantity $(\bar{u}Z)_{max}$ at the overshoot boundary are presented in figure 20. This quantity is proportional to G_{max}. At overshoot a good approximation for the constants developed in appendix A would be $C_q=0.6$ for positive lift, $C_q=0.7$ for zero lift, and $C_q=0.8$ to 0.9 for negative lift, as may be deduced from the table following equation (A13). Actually, heating rates are not relatively severe at overshoot, as may be judged from the fact that most of the values of $(\bar{u}Z)_{max}$ in figure 20 are considerably smaller than

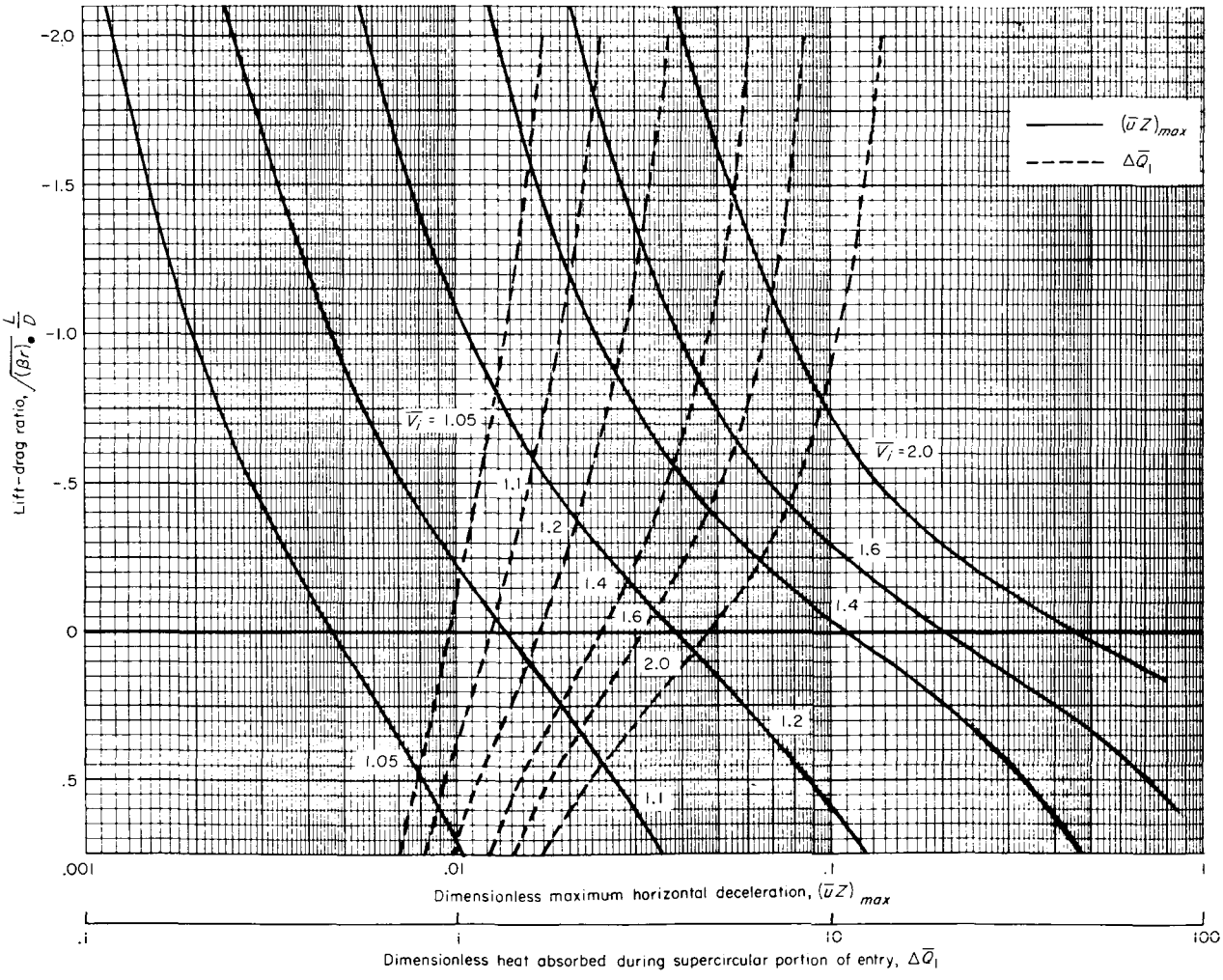

FIGURE 20.—Dimensionless maximum deceleration and laminar heat absorbed during supercircular portion of entry along overshoot boundary ($\bar{V}_{ex}=1$).

the value $(\overline{u}Z)_{max}=0.28$ representing orbital decay of a nonlifting satellite.

Near the overshoot boundary the total heat absorbed can become rather large, especially if negative lift is employed. The severity of this problem may be judged by comparison of relative values of the dimensionless quantity $\overline{Q}$, since the total heat absorbed is proportional to $\overline{Q}$ for a given planet and given vehicle (see eq. (A10)). Some approximate reference values are, $\overline{Q}=0.29$ for an ICBM entry ($\overline{V}_i=0.9$, $\gamma_i=24°$) and $\overline{Q}=1.1$ for nonlifting entry of a manned satellite ($\overline{V}_i=1$, $\gamma_i=2°$). A vehicle with $L/D=-1$ entering at parabolic velocity along the overshoot boundary would absorb during the supercircular portion of entry ($1<\overline{V}\leq\overline{V}_i$) an increment $\Delta\overline{Q}_1=4.7$. To this value must be added an increment $\Delta\overline{Q}_2\cong 1.1$ for the heat absorbed during the subcircular portion of entry. By comparison it follows that, for the same values of m/C_DA and nose radius R, the total heat absorbed along an overshoot-boundary entry ($\overline{Q}=5.8$) would be about 20 times that for an ICBM-type entry, and about 5 times that for a manned satellite-capsule entry.

Curves for various $\overline{V}_i$ and L/D are included in figure 20 representing the increment $\Delta\overline{Q}_1$ of laminar heat absorbed during the supercircular portion of entry along the overshoot boundary. For entry between the overshoot and undershoot boundaries the approximation of equation (A16),

$$\overline{Q}=\frac{\overline{u}_i^{\,3}\left(g_\oplus\sqrt{\beta r}\right)^{1/2}\left[1+\left(\overline{L/D}\right)^2\right]^{1/4}}{4C_Q\sqrt{G_{max}}} \tag{34}$$

is useful. This approximation would also apply to the subcircular portion alone by setting $\overline{u}_i=1$.

Aerodynamic heating at undershoot boundary.— Although the use of aerodynamic lift, particularly modulated L/D, can increase markedly the single-pass corridor width by lowering the undershoot boundary, this potential benefit is not obtained without a major penalty. Aerodynamic heating becomes progressively more severe as L/D is increased because of the low drag associated with high L/D. Both the rate of heating (eq. (A13)) and the total heat absorbed (eq. (A14)) vary inversely with C_D, the variation being as $C_D^{-0.5}$ for laminar convection, and as $C_D^{-0.8}$ for turbulent convection. Thus, for a given deceleration at undershoot, an entry with L/D maintained constant at 4 and $C_D/C_{D_{max}}=0.0065$ (see fig. 11) would experience laminar heating $(0.0065)^{-0.5}=12$ times as severe as one with $L/D=0$ and $C_D/C_{D_{max}}=1$; the relative turbulent heating would be $(0.0065)^{-0.8}=56$ times as severe.

If a constant $L/D=(L/D)_{entry}$ is employed near undershoot only until $\gamma\cong 0$, corresponding to a local minimum in altitude, and then L/D is reduced to 0 (or to small negative values) as the altitude begins to increase, entry can be completed and the net heat absorbed would not be as great as if the initial $(L/D)_{entry}$ were employed throughout. For parabolic entry, only about a third or less of the total heat would be absorbed up to the point where $\gamma=0$. Most of the heat would be absorbed during the subsequent monitoring phase wherein L/D is generally between 0 and $(L/D)_{entry}$. In order to estimate the total heat absorbed we will take for the average C_D during entry that corresponding to an L/D of (2/3) $(L/D)_{entry}$, and will consider both the case of operation in the high-drag portion of the drag polar (where C_D increases as L/D decreases) and operation in the low-drag portion (where C_D decreases as L/D decreases). Tabular values which follow illustrate the relative heating for various $(L/D)_{entry}$.

$(L/D)_{entry}$	High-drag portion of polar		Low-drag portion of polar	
	Laminar $Q/(Q)_{C_{D_{max}}}$	Turbulent $Q/(Q)_{C_{D_{max}}}$	Laminar $Q/(Q)_{C_{D_{max}}}$	Turbulent $Q/(Q)_{C_{D_{max}}}$
0	1.0	1.0	1.0	1.0
.5	1.2	1.3	1.8	2.6
1	1.3	1.5	2.9	5.5
2	2.2	3.6	6.9	22
3	3.4	7.0	12	52
4	5.0	13	18	100

As would be expected, the net heating penalities for high-drag monitoring with $(L/D)_{entry}=4$, for example, as represented by the factors of 5 for laminar convection and 13 for turbulent, are undesirably large but still much smaller than the corresponding factors mentioned previously of 12 and 56 applicable if L/D were equal to 4 throughout entry. These latter two factors, in turn, are smaller than the corresponding factors of 18 and 100 applicable for low-drag monitoring with $(L/D)_{entry}=4$.

An entry in which L/D is constant until $\gamma \cong 0$ and then is slowly reduced after the altitude begins to increase can operate in the high drag portion of the drag polar without further increasing the maximum deceleration beyond that experienced at $\gamma \cong 0$. It would be necessary, though, to decrease L/D slowly enough during the monitoring phase so that the accompanying increase in G due to increasing C_D is no greater than the aggregate effect of the decrease in G due to decreasing L/D and decreasing ρV^2.

It is unfortunate that the technique of modulated lift, which is so effective in broadening the entry corridor if a high $(L/D)_{\text{entry}}$ is employed and if C_D were maintained constant during modulation (as in curve D, fig. 12), would have its basic purpose defeated if the lifting vehicle attempted the modulation by operating in the high-drag portion of a polar (as in curve B, fig. 12). To see this, we note that the differential of the resultant deceleration $G = C_D \rho V^2 A \sqrt{1+(L/D)^2}/2mg_e$ is

$$\frac{dG}{G} = \frac{(L/D)d(L/D)}{1+(L/D)^2} + \frac{d(\rho V^2)}{\rho V^2} + \frac{dC_D}{C_D} \qquad (35)$$

During the monitoring phase $d(L/D)$ is negative, so that the first term on the right side represents the alleviation in G due to the reduction in transverse lifting force; the second term represents the change in G due to changing dynamic pressure; the third term, which was not considered in reference 1, represents the change in G due to changing C_D. For lifting surfaces operating in the high drag portion of the polar (curve B in figure 12), the increase in G due to increasing C_D is, unfortunately, about 3 times the decrease in G due to the reduction in transverse lift, so that modulation would result in a net loss, rather than a gain. This may be illustrated by considering the change in G per unit reduction in L/D at $L/D=1$. The change in G due to lift modulation alone, as given by the first term on the right side of equation (35), would be

$$\left(\frac{\Delta G}{G}\right)_{\text{lift variation}} = \frac{L/D}{1+(L/D)^2}\,\Delta\left(\frac{L}{D}\right) = \frac{1}{1+1}(-1) = -\frac{1}{2}$$

which represents a reduction in deceleration. The accompanying change in G due to drag variation as given by the third term together with the top curve in figure 11 would be

$$\left(\frac{\Delta G}{G}\right)_{\text{drag variation}} = \frac{\Delta C_D}{C_D} = \frac{0.73-0.17}{0.35} = 1.6$$

which represents an increase in deceleration due to drag variation amounting to over three times the decrease due to lift variation. It follows that drag modulation through α variation of a *lifting* vehicle would be more effective than lift modulation through L/D variation in broadening the entry corridor. Drag modulation of this type is not investigated herein; drag modulation of *nonlifting* vehicles has been studied recently by Phillips and Cohen in reference 6.

If, rather than to change angle of attack of a lifting surface, the aerodynamic technique of deploying a drag device were employed to reduce L/D (such as represented by curve C in fig. 12), then the adverse effect of increasing drag would still exceed the favorable effect of decreasing L/D. The full benefits of modulated L/D can be realized, however, by operating a lifting surface in the low drag portion of the polar (such as represented by curve A, in fig. 12), but then very large heating penalties would result, as exemplified by the numbers listed in the right half of the above table. The use of any modulation technique which requires that the vehicle operate along the low drag portion of its polar will necessarily be penalized severely by aerodynamic heating in comparison to the constant L/D technique which can be used with the vehicle operating along the high drag portion of the polar.

The complicated trade-off between guidance benefits and aerodynamic heating penalties is further slanted toward the use of only small or moderate L/D, rather than higher L/D, by the role which boundary-layer transition may play. That transition may play an important role can be seen from a comparison of two cases: (1) constant L/D with $(L/D)_{\text{entry}}=1$, and (2) modulated L/D with $(L/D)_{\text{entry}}=4$. The guidance benefit associated with case (2) amounts to a parabolic entry corridor about 3 times as broad as for case (1). In assessing the accompanying heating penalty, let us first estimate the Reynolds number of a hypothetical manned spacecraft. For both cases we take $l=50$ feet, $m/A=1$ slug per square foot, $G_{max}=10$, and $\overline{V}=1.2$. From equation (A7) we have, for the earth's atmosphere

$$\frac{Re}{l} = \frac{7700}{\sqrt{1+(L/D)^2}}\,\frac{G}{\overline{V}}\left(\frac{m}{C_D A}\right) \qquad (36)$$

Hence, for case (1) with $(L/D)_{\text{entry}}=1$ and $C_{D_{av}}=1$ (corresponding to operation in the high-drag por-

tion of the polar with $(L/D)_{av}=(2/3)\ (L/D)_{entry}$), there results $Re=3\times10^6$ at which value considerable laminar flow would be expected; from the above table the heating penalty would be 1.3 times that for laminar flow with $L/D=0$. For case (2) with $(L/D)_{entry}=4$ and modulation at $C_D=0.011$ (corresponding to operation at a constant C_D equal to that at $L/D=4$), there results $Re=100\times10^6$ at which value mostly turbulent flow would be expected; the heating penalty would be 100 times that for turbulent flow with $L/D=0$. Since the Stanton number for turbulent flow is at least several times that for laminar, the net heating-penalty factor would be at least several times 100/1.3, which would amount to well over a factor of 100. This appears too great a heating penalty to pay for the guidance benefits of a tripled Earth corridor width. For entry into Mars, though, a one-hundredfold increase in heating may be manageable, but in this case the corridor already is relatively broad even for nonlifting vehicles.

As L/D is increased from 0, the increase in heating penalty is slow at first for modes of entry which utilize the high drag portion of a polar. Up to about $L/D\cong1$ the associated heating penalty would not appear to limit appreciably the usefulness of aerodynamic lift in broadening the entry corridor. For entry at parabolic velocity, the 10 G Earth corridor for $(L/D)_{entry}=1$ is 7.6 times as wide as for $L/D=0$, whereas the laminar heat absorbed need be increased only about 30 percent. The trade-off between guidance benefit and heating penalty would appear to favor the lifting vehicle at least up to about $L/D=1$. In this range of L/D, modulated L/D would not be much more effective in widening the corridor than constant L/D, and would have somewhat greater heating. When both guidance and heating problems are considered, a compromise single-pass entry technique would be to enter with a value of L/D the order of unity until maximum deceleration is experienced, then reduce L/D in the high-drag attitude (increasing α) until intense heating is over, and, finally, increase L/D again (decreasing α) to achieve maximum maneuverability in the terminal glide phase. As previously indicated, the technique (not studied) of drag modulation of a lifting vehicle by reducing α before $\gamma=0$ and alleviating G through the decrease in C_D with increasing L/D, could be more efficient in broadening the corridor than the technique of lift modulation; it is to be noted, however, that this technique also would require operation in the low drag portion of a polar with the accompanying heating penalty (although the penalty would not be so severe as for lift modulation).

Different heating problems at undershoot and overshoot.—In relation to the status of current technology, the rate of aerodynamic heating along the undershoot boundary is quite high. For example, if $\overline{u}=1.3$, $\sqrt{\beta r}=30$, $G_{max}=10$, and $L/D=0.5$, equation (A13) yields for the maximum dimensionless heating rate $\overline{q}_{max}=0.92$, which is much higher than the corresponding value $\overline{q}_{max}=0.22$ for a satellite in orbital decay, and considerable higher even than the value $\overline{q}_{max}=0.62$ for a typical ICBM entry. Since $(\overline{q}_{max})^{1/4}$ is proportional to the maximum wall temperatures, this temperature for a vehicle that is entirely radiation-cooled during parabolic entry at undershoot would be about 10 percent higher than in an ICBM entry. Surface temperatures sufficient for radiation cooling of an ICBM nose cone currently are not considered to be practically feasible, and similarly are not considered feasible currently for a spacecraft entering near the undershoot boundary.

The total heat absorbed along the undershoot boundary, however, is not excessively high. For example, if L/D is monitored so as to decelerate at an essentially constant value of 8 G, then equation (34) yields (with $\overline{u}_i=1.4$, $\sqrt{\beta r}=30$, $\overline{L/D}=0.5$, and $C_Q=\frac{3}{4}$) the value $\overline{Q}_{un}=1.9$. This is not discouragingly larger than the value $\overline{Q}=1.1$ representative of a nonlifting manned satellite entering from a near circular orbit, for which the technique of absorption by ablation appears eminently practical at present. The value $\overline{Q}_{un}=1.9$ is, however, only about $\frac{1}{3}$ of the corresponding value $\overline{Q}_{ov}=5.8$ for entry along the overshoot boundary.

In summary, then, we are faced with a situation wherein at the deceleration-limited undershoot of the Earth corridor, the heating rate is relatively large, and pure radiation cooling currently appears impractical, but the total heat absorbed is within practical bounds of present heat-absorption techniques; at overshoot, however, the heating rate is relatively small, pure radiation cooling appears practical, but the total heat absorbed is about 3 times that at undershoot. For an efficient design, therefore, it is important to develop versatile

protection shields which can radiate efficiently if a spacecraft enters near overshoot, ablate efficiently if it enters near undershoot, and blend these functions efficiently if it enters anywhere in between.

EXAMPLE GUIDANCE REQUIREMENTS FOR ENTRY CORRIDORS OF VARIOUS PLANETS

In order to determine the desired trajectory which passes along the center of an entry corridor it would be necessary to make precise three-dimensional orbit calculations giving full consideration to a number of perturbations such as those due to planetary oblateness, the sun, moon, and perhaps other planets. In calculating the small deviations about this desired center-line trajectory which are permissible from atmosphere entry considerations, however, the secondary effects of the perturbations on these small deviations will be disregarded, and the entry guidance tolerances calculated as those of a two-body problem. This procedure appears reasonable inasmuch as the terminal-guidance correction to an entry approach would presumably be made relatively near the target planet where the trajectory is mainly in one plane and is essentially a conic trajectory. Results of such calculations should be useful, for example, in making preliminary estimates of what distance from a target planet would be optimum for correcting a trajectory, how much fuel would be expended in so doing, and whether certain types of supercircular entry maneuvers would be feasible from a viewpoint of the guidance accuracy they impose.

By the use of equation (22) for narrow corridors (Earth, Venus, Jupiter) and the full equation (20) for relatively broad corridors (Mars, Titan), the guidance requirements on $\pm\Delta\gamma$ (permissible deviation from the flight-path angle of the trajectory which passes through the center of the entry corridor) for zero errors in $\overline{V}$ and r have been determined for the various 10 G_{max}, parabolic-entry corridors previously considered. Values of $\pm\Delta\gamma$ are plotted in figure 21 as a function of the dimensionless distance r/r_0. It is evident that the $\pm\Delta\gamma$ requirements vary by large amounts, from the order of 10° for Titan to less than 0.01° for Jupiter. For comparison, three other technological requirements (also computed for zero error in V) are indicated for reference immediately to the right of the $r/r_0=100$ line. They are: $\pm 2°$ for injecting a vehicle into orbit around the earth, $\pm 0.25°$ for hitting the moon from the earth (ref. 7), and $\pm 0.014°$ for ± 1 mile ICBM accurancy at 5000 miles range (this is the azimuthal angle requirement; the corresponding flight-path-angle requirements are less severe). At the far right of the figure are indicated three different approximate guidance requirements which, though more mundane, nevertheless are fully as illuminating and nearly as stringent as the three technological requirements. It is seen that, starting at $r/r_0=100$, it would require no better angular guidance control (1) to enter the corridor of Titan than to inject a satellite into orbit or to pitch a baseball strike; (2) to enter the corridor of Mars than to hit the moon from the earth or to hit an apple from 60 feet (William Tell), or, (3) to enter the corridors of Venus and Earth than to launch an ICBM within azimuthal accuracy of 1/5000 of the range, or to fire a rifle within bull's-eye target accuracy (accomplished essentially 100 percent of the time by skilled individuals). To aline a trajectory for entry into Jupiter, however, is another matter.

The corresponding requirements on velocity control $\pm\Delta\overline{V}/\overline{V}$ for zero error in γ and r also have been calculated, with the following results (descending vertically in order of increasing severity).

Parabolic entry 10 G corridor	$\pm\Delta\overline{V}/\overline{V}$	Comparative technological requirements	$\pm\Delta\overline{V}/\overline{V}$
Titan	1.		
Mars	0.03		
		Orbit injection	0. 02
Venus	. 003		
Earth	. 003		
		Moon shot	. 001
Jupiter	. 0003		
		ICBM	. 00004

The parabolic entry requirements on $\pm\Delta\overline{V}/\overline{V}$ for Earth and Venus are less severe than successful Moon-shot requirements, and two orders of magnitude less than ICBM requirements. In fact, to put these requirements in perspective, the velocity control required for Venus and Earth is not much more severe than the velocity control with which a skilled man can throw a ball. In the Italian game of boccie ball, for example, a skilled player often throws a 4-inch wooden ball about 30 feet to hit another similar ball (without hitting nearly adjacent ones), and this requires $\pm\Delta\overline{V}/\overline{V}\cong 0.006$, which is comparable to the

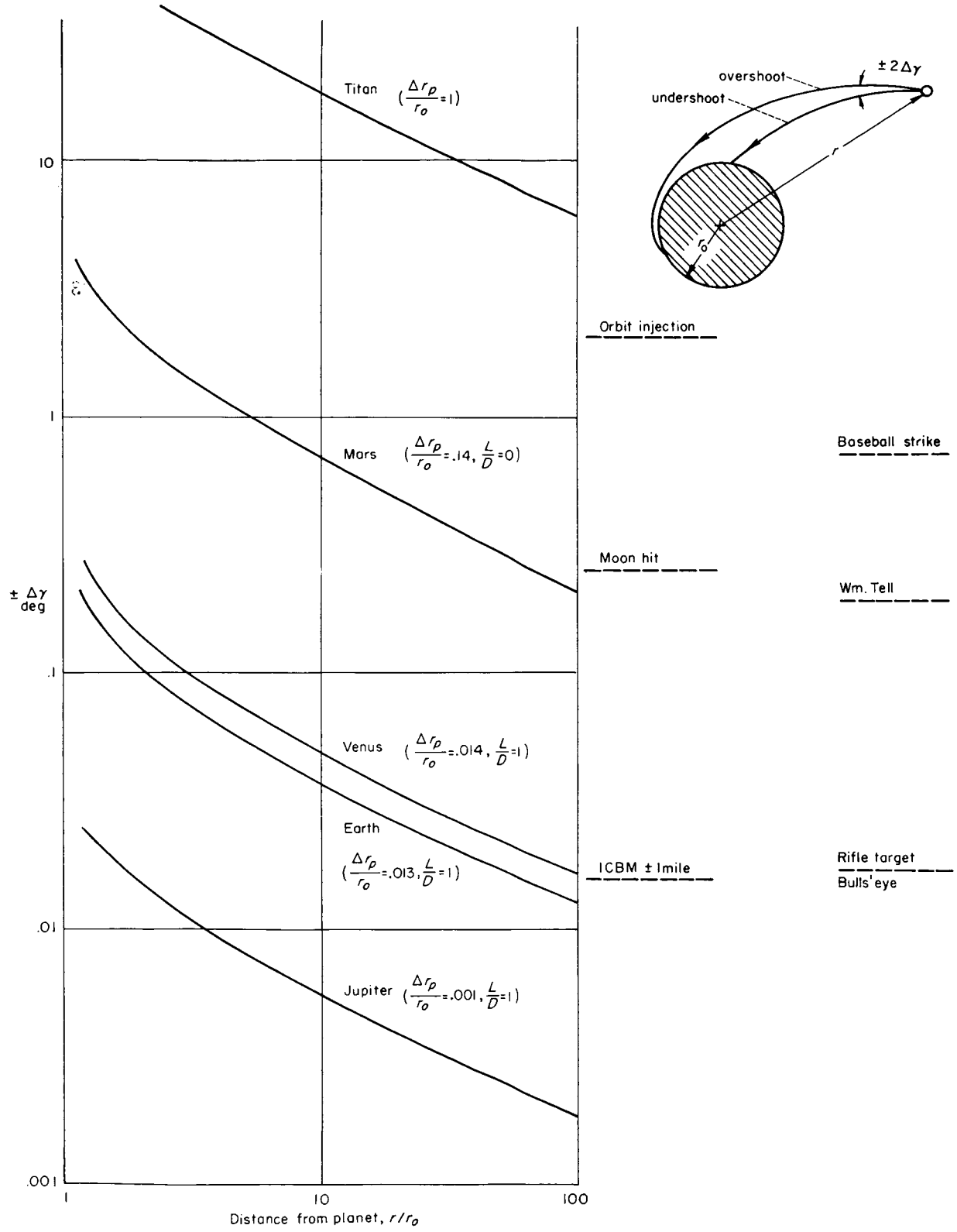

FIGURE 21.—Guidance accuracy requirements on flight path angle for single-pass 10 G_{max} parabolic entries, and comparison with other guidance requirements.

value ± 0.003 for parabolic entry into Venus or Earth. In general the entry requirements for velocity control do not appear as severe, relatively speaking, as those for flight-path-angle control.

The permissible errors in distance from the planet $\pm \Delta r/r$ for zero errors in $\overline{V}$ and γ, are seen from equation (22) to be equal to $\pm 2\Delta\overline{V}/\overline{V}$. Only in the extreme case of Jupiter ($\pm \Delta r/r = 0.0006$) would distance errors appear to impose any really severe requirement or precise knowledge of distance from the planet center.

RESUMÉ OF RESULTS

A dimensionless, transformed, nonlinear differential equation previously developed for describing motion during entry into a planetary atmosphere has been combined with equations for conic trajectories to yield a parameter ($F_p = \rho_p \sqrt{r_p/\beta}/2(m/C_D A)$) based on conditions at the conic perigee altitude which is convenient for specifying the width and altitude of an entry corridor. The width of a deceleration-limited corridor in an exponential atmosphere is independent of $m/C_D A$, but the density ρ_p at conic perigee is proportional to $m/C_D A$.

The corridor width decreases markedly as the entry velocity increases. For example, the 10 G_{max} corridor width for entry of nonlifting vehicles into the earth's atmosphere decreases from about 180 miles for circular entry ($\overline{V}_i = 1$), to 7 miles for parabolic entry ($\overline{V}_i = \sqrt{2}$), to 0 miles for hyperbolic entry at $\overline{V}_i = 1.8$. As would be anticipated, the corridor width for a given entry $\overline{V}_i$ into various objects in the solar system varies by large amounts, ranging from a minute fraction of the radius for Jupiter, to the full radius for Titan.

The overshoot boundary of an entry corridor can be extended upward by the use of negative lift, but only about one $\log_{10}$ cycle in F_p (or in density). Deployment of a large, light, drag device appears to be a much more effective way to raise the overshoot boundary.

The undershoot boundary of the entry corridor can be lowered markedly by the use of aerodynamic lift, and lowered more by modulated L/D than by constant L/D. This is in agreement with previous results of Lees, Hartwig, and Cohen who did not consider any inherent C_D-L/D dependence. The benefits of modulated lift in alleviating guidance requirements, however, are sizable only for relatively large L/D ratios (greater than about 1) which inherently require low C_D and much more heat to be absorbed than for small L/D. When the strong C_D-L/D interdependence for lifting surfaces is considered, the modulated L/D technique appears restricted to operation in the low-drag portion of a drag polar (where C_D decreases as L/D decreases), and thus penalized by much higher heating rates than the constant L/D technique which can utilize the high-drag portion of a drag polar (where C_D increases as L/D decreases). Because of the strong C_D-L/D coupling of a lifting surface, the decrease in C_D with decreasing angle of attack can overshadow the accompanying variation in resultant force with changing L/D, so that drag modulation by variation in angle of attack of a lifting vehicle would appear to be more effective in lowering the undershoot boundary of a deceleration-limited corridor than would be lift modulation.

A compromise technique for single-pass supercircular entry, considering both guidance and heating problems, is to employ initially a constant L/D (of about 1 if entry is near undershoot, or less if the conic perigee is higher) until slightly past maximum deceleration, then reduce L/D to essentially 0 (or to small negative values if entry is near overshoot) by increasing the angle of attack in the high-drag portion of the drag polar until intense heating is over and single-pass entry is assured, and finally to increase L/D again so that maximum maneuverability is achieved during the terminal glide phase.

Because of the opposite nature of the aerodynamic heating problems at overshoot (high total heat absorbed, low heating rates) and undershoot (low total heat absorbed, high heating rates), it is highly desirable to develop versatile protection shields for spacecraft which can radiate efficiently if entry happens to occur near overshoot, ablate efficiently if near undershoot, and blend these characteristics if entry occurs in between.

Compared to other technological guidance requirements, such as those for successful Moon shots from the Earth, or for achieving an accuracy in azimuthal angle for an ICBM of 1 part in 5000, the entry-corridor requirements imposed on flight path angle appear to be relatively more severe

than those imposed on velocity. For parabolic entry into the earth's atmosphere, the limitations on flight path angle are about the same as those of the comparison ICBM requirement.

As far as terminal entry guidance is concerned, it appears feasible to employ the atmosphere of certain planets—rather than rocket fuel—to effect orbital transfers wherein a spacecraft approaching a target planet at hyperbolic velocity has its trajectory converted by atmosphere drag to an elliptic orbit about that planet. The corridor width for such maneuvers is not impractically narrow if the vehicle possesses the intelligence capability of accurately knowing which trajectory within the corridor it is approaching upon, together with the monitoring capability of being able to program L/D (and C_D) in the variety of ways required for different approaches within the corridor boundaries. The apparent feasibility of atmosphere braking for effecting hyperbolic-elliptic orbital transfers implies the possibility of very large reductions in Earth lift-off weight for interplanetary voyages employing chemical propulsion.

Some typical 10 G_{max} entry corridor widths, expressed as a fraction $\Delta y_p/r_0$ of the planet radius, are tabulated here for convenience. All correspond to lifting vehicles with an L/D capability of about 1, unless specifically noted otherwise.

	$\Delta y_p/r_0$
Parabolic entry into Titan ($L/D=0$)	1.
Mars ($L/D=0$)	. 26
Venus	. 015
Earth	. 013
Earth ($L/D=0$)	. 002
Jupiter	. 001
Atmosphere braking for minimum heating rates into Earth	. 0005
Atmosphere braking for converting Earth parabolic approach into elliptical orbit with apogee altitude less than 1000 miles, and simultaneously not exceeding 10 G_{max}:	
(variable L/D programing)	. 01
(fixed $L/D \cong 0.5$)	. 002
Atmosphere braking for heliocentric-planetocentric orbital transfer:	
Into Mars from Earth (variable L/D programing)	. 17
Into Mars from Earth (fixed L/D)	. 12
Into Earth from Mars (variable L/D programing)	. 012
Into Earth from Mars (fixed $L/D \cong 0.4$)	. 007
Into Earth from distant point in solar system (variable L/D programing)	. 004

AMES RESEARCH CENTER
NATIONAL AERONAUTICS AND SPACE ADMINISTRATION
MOFFETT FIELD, CALIF., *Aug. 5, 1959*

APPENDIX A

FORMULAS FOR MOTION AND HEATING QUANTITIES AND RELATIONSHIP BETWEEN DECELERATION AND HEATING

FORMULAS FOR MOTION AND HEATING QUANTITIES RELATED TO Z

The full form of the differential equation for Z developed in reference 2 is:

$$\bar{u}\frac{d^2Z}{d\bar{u}^2}-\left(\frac{dZ}{d\bar{u}}-\frac{Z}{\bar{u}}\right)=\frac{1-\bar{u}^2}{\bar{u}Z}\cos^4\gamma-\sqrt{\beta r}\,\frac{L}{D}\cos^3\gamma \quad \text{(A1)}$$

Here, and in the equations which follow, the appropriate form for shallow entries is obtained by setting $\cos\gamma=1$, $\sin\gamma=\gamma$, and by disregarding $L/D\tan\gamma$ and $\tan^2\gamma$ compared to unity. Equations for various quantities of interest related to Z are (their derivation may be found in ref. 2):

Flight-path angle

$$\sqrt{\beta r}\sin\gamma=\frac{dZ}{d\bar{u}}-\frac{Z}{\bar{u}} \quad \text{(A2)}$$

Horizontal deceleration

$$-\frac{du}{dt}=\frac{g\sqrt{\beta r}\,\bar{u}Z}{\cos\gamma} \quad \text{(A3)}$$

Resultant deceleration

$$a=\frac{g\sqrt{\beta r}\,\bar{u}Z}{\cos\gamma}\sqrt{1+\left[\left(\frac{L}{D}\right)-\tan\gamma\right]^2} \quad \text{(A4)}$$

Range between $\bar{u}_i$ and $\bar{u}$

$$\sqrt{\beta r}\,\frac{s-s_i}{r}=\int_{\bar{u}_i}^{\bar{u}}\frac{\cos\gamma\,d\bar{u}}{Z} \quad \text{(A5)}$$

Density-velocity relationship

$$\rho=2\left(\frac{m}{C_DA}\right)\sqrt{\frac{\beta}{r}}\,\frac{Z}{\bar{u}} \quad \text{(A6)}$$

Reynolds number per unit length

$$\frac{Re}{l}=\frac{2\sqrt{g\beta}}{\mu\cos\gamma}\left(\frac{m}{C_DA}\right)Z \quad \text{(A7)}$$

For either laminar or turbulent flow, a convenient reference rate for convective heating into a surface of radius of curvature R can be represented by the equation

$$q=\frac{C}{R^{1-n}}\rho^nV^3 \quad \text{(A8)}$$

Approximate values of C for air, with ρ in slugs per cubic foot, R in feet, and V in feet per second are listed below together with the values of n for laminar and turbulent flow.

	For q in Btu ft^{-2}sec^{-1}	
Reference heating rate	C	n
Laminar stagnation point (ref. 2)	2.0×10^{-8}	$\frac{1}{2}$
Turbulent sonic point (ref. 8)	9.0×10^{-6}	$\frac{4}{5}$

By combining this equation with the density-velocity relationship (A6) we have, for the case of shallow entry:

heating rate

$$q=\frac{2^nC}{R^{1-n}}\left(\frac{m}{C_DA}\right)^n\left(\beta^{\frac{n}{2}}r^{\frac{3-n}{2}}g^{\frac{3}{2}}\right)\bar{q} \quad \text{(A9)}$$

where

$$\bar{q}\equiv\bar{u}^{3-n}Z^n \quad \text{(A9a)}$$

total heat absorbed per unit area

$$\frac{Q}{S}=\frac{2^nC}{R^{1-n}}\left(\frac{m}{C_DA}\right)^n\left(\beta^{\frac{n-1}{2}}r^{\frac{3-n}{2}}g\right)\bar{Q} \quad \text{(A10)}$$

where

$$\bar{Q}\equiv\int_0^{\bar{u}_i}\frac{\bar{u}^{3-2n}d\bar{u}}{(\bar{u}Z)^{1-n}} \quad \text{(A10a)}$$

At a laminar stagnation point in air, these two equations become (with m/C_DAR in slug ft^{-3})

$$q_s=590\sqrt{\frac{m}{C_DAR}}\,\bar{q}\,\frac{\text{Btu}}{\text{ft}^2\text{sec}} \quad \text{(A11)}$$

with

$$\bar{q}=\bar{u}^{5/2}Z^{1/2} \quad \text{(A11a)}$$

and

$$\frac{Q_s}{S}=15{,}900\sqrt{\frac{m}{C_DAR}}\,\bar{Q}\,\frac{\text{Btu}}{\text{ft}^2} \quad \text{(A12)}$$

with

$$\overline{Q}=\int_0^{\overline{u}_i}\frac{\overline{u}^{3/2}d\overline{u}}{\sqrt{\overline{Z}}} \qquad \text{(A12a)}$$

The quantities $\overline{q}$ and $\overline{Q}$ are referred to as the dimensionless heating rate and the dimensionless total heat absorbed, respectively. In atmospheres of planets other than Earth, additional factors $q_\oplus$ and $Q_\oplus$, not considered herein, appear on the right sides of equations (A11) and (A12), respectively, representing the relative aerodynamic heating compared to that in the earth's atmosphere. These factors for laminar convection are estimated in reference 2 for Venus, Mars, and Jupiter.

APPROXIMATE HEATING-DECELERATION RELATIONSHIPS

Approximate relationships developed below between convective heating and deceleration are employed later to assist in explaining certain qualitative results, and in evaluating the aerodynamic heating problem for different portions of the entry corridor. By combining equations (A3) for deceleration and (A9) for rate of heating, there results a general qualitative relationship applicable to a given planet (the constant of proportionality depends on the planet).

$$q\sim\frac{1}{R^{1-n}}\left(\frac{m}{C_DA}\right)^n\overline{u}^{3-2n}(\text{deceleration})^n \qquad \text{(A13)}$$

Through the use of a mean value approximation for integrals, equations (A10) and (A10a) for total heat absorbed from $\overline{u}_i$ to $\overline{u}=0$ yield

$$\frac{Q}{S}\sim\frac{1}{R^{1-n}}\left(\frac{m}{C_DA}\right)^n\frac{\overline{u}_i^{4-2n}}{(\text{mean deceleration})^{1-n}} \qquad \text{(A14)}$$

Except for the case $n=1$ (e.g., free-molecule flow) these relationships show that the greater the deceleration the greater the heating rate, but the smaller the total heat absorbed.

The qualitative heating-deceleration relationships can be put on a quantitative basis. During the supercircular portion of an entry, maximum heating rate and maximum deceleration occur reasonably close together. If $\overline{u}$ at maximum heating rate is written as $C_q\overline{u}_i$, where C_q is a constant somewhat less than unity, then equations (A11a), (A3), and (A4) yield an approximate—though general—relationship for laminar convection.

$$\overline{q}_{max}=(C_q\overline{u}_i)^2\sqrt{(\overline{u}\overline{Z})_{max}}=\frac{(C_q\overline{u}_i)^2\sqrt{\overline{G}_{max}}}{(g_\oplus\sqrt{\beta r})^{1/2}[1+(L/D)^2]^{1/4}} \qquad \text{(A15)}$$

Values of C_q for laminar heating fall in the range $0.6<C_q<1$, as indicated by the following values determined from both analytical (when in parentheses) and numerical results of reference 2:

Type of entry			C_q
Orbital decay from $\overline{V}_i=1$ with $L/D=0$			0.64
		1	.64
		∞	.62 $(=\sqrt{2/3\sqrt{3}})$
Steep entry from any $\overline{V}_i$ with $L/D=0$			.76 $(=3^{-1/4})$
Undershoot entry with $L/D=0$			.80
		1	.90
		∞	1.00
Overshoot-limit entry with $L/D=0$	from $\overline{V}_i=1.2$ to	$\overline{V}_f=1$	.64
	1.4	1	.67
	2.0	1	.73
Overshoot-limit entry with $L/D=-1$	from $\overline{V}_i=1.2$ to	$\overline{V}_f=1$	.78
	1.4	1	.86
	2.0	1	.92

For the extreme case of negligible, but constant horizontal deceleration ($\overline{u}Z=\text{const}\to 0$), maximum heating will occur at the initial point, so that $C_q\to 1$ in this limiting case.

An analogous approximation can be established for the dimensionless laminar heat absorbed $\Delta\overline{Q}$ during entry from $\overline{u}_i$ to $\overline{u}_f$. By employing a mean value approximation for integrals, we have from equations (A12a), (A3), and (A4),

$$\Delta\overline{Q}=\left(\frac{\overline{u}_i+\overline{u}_f}{2}\right)^2\frac{(\overline{u}_i-\overline{u}_f)}{C_Q\sqrt{(\overline{u}\overline{Z})_{max}}}$$

$$=\frac{(\overline{u}_i+\overline{u}_f)^2(\overline{u}_i-\overline{u}_f)}{4C_Q\sqrt{G_{max}}}(g_\oplus\sqrt{\beta r})^{1/2}[1+(\overline{L/D})^2]^{1/4} \qquad \text{(A16)}$$

Values of C_Q for laminar convection generally are in the range $0.32<C_Q<1$, as may be deduced from the following results:

Type of entry	C_Q
Orbital decay from $\overline{u}_i=1$ to $\overline{u}_f=0$ with $L/D=\infty$	0.32 $(=1/\pi)$
Steep entry from $\overline{u}_i$ to 0 with $L/D=0$	.46 $(=\sqrt{e}/2\sqrt{\pi})$
Shallow skip from $\overline{u}_i$ to $\overline{u}_f$, $\overline{u}_i$ with $L/D=\infty$	.64 $(=2/\pi)$
Overshoot-limit entry with $L/D=0$ from $\overline{u}_i=2.0$ to $\overline{u}_f=1$	.70
1.4 1	.72
Overshoot-limit entry with $L/D=-0.5$ from $\overline{u}_i=2.0$ to $\overline{u}_f=1$	.74
1.4 1	.77
{Constant horizontal deceleration with arbitrary L/D from $\overline{u}_i$ to 0}	.75

for the limiting case of constant horizontal deceleration during a negligible velocity decrement (the case when $\overline{u}Z$ is a Dirac function of $\overline{u}$), $C_Q=1$.

The approximate heating-deceleration relationships for complicated types of entry agree well with more precise calculations, and illustrate that, in an entry wherein the deceleration is monitored to be essentially constant, the aerodynamic heating with a fixed m/C_DA does not depend significantly on the lift-drag ratio. Lees, Hartwig, and Cohen (ref. 1) have made machine calculations of an entry wherein L/D is varied continuously after reaching G_{max} in the particular manner which maintains constant resultant deceleration and constant C_D. For this type of modulated lift they used the numerical values $m/C_DA=3.1$ slugs per square foot, $V_i=35{,}000$ feet per second $(\overline{V}_i=1.36)$, and $G_{max}=10$. Since this corresponds to an undershoot type of entry, we take $C_q=0.9$ from the table preceding the one above, and since the deceleration is constant for most of the entry, $C_Q=\frac{3}{4}$ from the above table. By substitution of these numerical values into equations (A11) and (A15) for q, and (A12) and (A16) (using $\overline{L/D}=\frac{1}{2}(L/D)_{\text{entry}}$) for Q, the results obtained are found to be in approximate agreement with the more accurate machine calculations of Lees, et al. The following table illustrates this for laminar stagnation heating with $R=1$ foot:

L/D at entry	Maximum heating rate, Btu ft^{-2}sec^{-1}		Total heat absorbed, Btu ft^{-2}	
	$q_{s_{max}}$ Eqs. (A11) and (A15)	$q_{s_{max}}$ Ref. 1	Q_s/S Eqs. (A12) and (A16)	Q_s/S Ref. 1
0. 25	890	780	41, 000	40, 000
. 5	840	800	41, 000	39, 000
1	760	810	43, 000	39, 000

It is noted here that the above tabular values, which indicate only minor variations in heating with $(L/D)_{\text{entry}}$ for essentially the same deceleration history, assume that m/C_DA is constant for all values of L/D; calculations presented elsewhere in this report consider a variation of C_D with L/D and show a large dependence of heating on L/D.

RELATIONSHIP BETWEEN DECELERATION AND REYNOLDS NUMBER

A useful equation relating Reynolds number per unit length to deceleration is obtained by combining equations (A4) and (A7)

$$\frac{Re}{l}=\frac{2g_e}{\mu\sqrt{rg}}\left(\frac{m}{C_DA}\right)\frac{G}{\overline{u}\sqrt{1+(L/D)^2}} \tag{A17}$$

$$=\frac{7700}{\mu_\oplus\sqrt{r_\oplus g_\oplus}}\left(\frac{m}{C_DA}\right)\frac{\overline{G}}{\overline{u}\sqrt{1+(L/D)^2}} \tag{A18}$$

This equation enables the maximum Reynolds number to be calculated approximately from G_{max} and an estimate of the value of $\overline{u}$ at which G_{max} is experienced.

APPENDIX B

INTERDEPENDENCE OF C_D AND L/D FOR LIFTING VEHICLES

The equations of Newtonian hypersonic flow for the case where lift is obtained by varying α of a surface enable a simple picture to be obtained of the L/D-C_D relationship. Let us designate the minimum drag coefficient at 0° angle of attack as C_{D_o}, and that at 90° as $C_{D_{max}}$. In accordance with Newtonian flow, pressures are assumed to vary as $\sin^2\alpha$, so that $C_D=C_{D_o}+(C_{D_{max}}-C_{D_o})\sin^3\alpha$; hence, this approximation yields

$$\frac{L}{D}=\frac{\sin^2\alpha\cos\alpha}{b+\sin^3\alpha} \tag{B1}$$

The quantity $b=C_{D_o}/C_{D_{max}}-C_{D_o})$ determines the maximum value of L/D and the α at which it occurs. Even for a flat plate having zero leading-edge radius, zero pressure drag at $\alpha=0$, and laminar skin friction, the $(L/D)_{max}$ in hypersonic Newtonian flow is only about 6 at a Reynolds number of 1 million. In view of this, and the severe heating problems associated with lifting surfaces having small leading-edge radii, we will confine our attention to $(L/D)_{max}$ of 4 or less. Four drag polars corresponding to values of b such that $(L/D)_{max}=1$, 2, 3, and 4, as determined by the above equation, are shown in figure 11 with L/D plotted versus $C_D/C_{D_{max}}$ (a value $C_{D_{max}}\cong 1.7$ would be reasonable for all of the polars). In each case L/D increases from 0 at the minimum drag attitude ($\alpha=0$), passes through a maximum, and then decreases to 0 again at the maximum drag attitude ($\alpha=90°$). The low C_D's associated with high L/D are evident from this figure.

The interdependence of C_D and L/D can be varied widely by employing different aerodynamic techniques, but we are most interested in the technique which gives maximum drag for a given L/D. A wide variation is illustrated in figure 12 where four different curves are shown, all starting from $(L/D)_{max}=4$. Curve A corresponds to varying the angle of attack in the low-drag portion of the drag polar of a lifting surface, while curve B corresponds to the high-drag portion of the polar. Curve C corresponds to varying the drag at constant lift, such as could be done by deploying a variable-area drag device while the lifting surface maintains a fixed C_L (referred to the fixed area of the lifting surface). Curve D corresponds to varying the lift at constant C_D (also referred to the same area) such as could be done by simultaneously changing α and deploying a variable-area drag device. Curve B, the high-drag portion of the polar, yields the highest C_D for a given L/D of the various curves considered (including those in fig. 11), and, therefore, would be best from the viewpoint of minimizing the aerodynamic heating. The relationship between L/D and C_D for this curve is:

L/D	$C_D/C_{D_{max}}$
0	1.00
.25	.92
.5	.73
1	.35
2	.087
3	.027
4	.0065

This particular interdependence of L/D and C_D is used herein to evaluate the net broadening of corridor width and the aerodynamic heating penalty associated with the use of lifting vehicles.

REFERENCES

1. Lees, Lester, Hartwig, Frederic W., and Cohen, Clarence B.: The Use of Aerodynamic Lift During Entry Into the Earth's Atmosphere. Space Technology Lab. Rep. GM–TR–0165–00519, Nov. 1958.
2. Chapman, Dean R.: An Approximate Analytical Method for Studying Entry Into Planetary Atmospheres. NACA TN 4276, 1958.
3. Nielsen, Jack N., Goodwin, Frederick K., and Mersman, William A.: Three-Dimensional Orbits of Earth Satellites, Including Effects of Earth Oblateness and Atmospheric Rotation. NASA Memo 12–4–58A, 1958.
4. Allen, H. Julian, and Eggers, A. J., Jr.: A Study of the Motion and Aerodynamic Heating of Missiles Entering the Earth's Atmosphere at High Supersonic Speeds. NACA TN 4047, 1957.
5. Eggers, Alfred J., Jr., Allen, H. Julian, and Neice, Stanford E.: A Comparative Analysis of the Performance of Long-Range Hypervelocity Vehicles. NACA TN 4046, 1957. (Supersedes NACA RM A54L10).
6. Phillips, Richard L., and Cohen, Clarence B.: Use of Drag Modulation to Reduce Deceleration Loads During Atmospheric Entry. Am. Rocket Soc. Jour., vol. 29, no. 6, June 1959, pp. 414–422.
7. Lieske, H. A.: Accuracy Requirements for Trajectories in the Earth-Moon System. Rand Rep. P–1022, Feb. 19, 1957.
8. Sibulkin, Merwin: Estimation of Turbulent Heat Transfer at the Sonic Point of a Blunt-Nosed Body. Jet Propulsion, vol. 28, no. 8, pt. I, 1958, pp. 548–554.

U.S. GOVERNMENT PRINTING OFFICE: 1961